
VCR: Visual Caption Restoration

Anonymous Author(s)

Affiliation

Address

email

Abstract

1 We introduce Visual Caption Restoration (VCR), a novel vision-language task that
2 challenges models to accurately restore partially obscured texts using pixel-level
3 hints within images. This task stems from the observation that text embedded in
4 images is intrinsically different from common visual elements and natural language
5 due to the need to align the modalities of vision, text, and text embedded in
6 images. While numerous works have integrated text embedded in images into
7 visual question-answering tasks, approaches to these tasks generally rely on optical
8 character recognition or masked language modeling, thus reducing the task to
9 mainly text-based processing. However, text-based processing becomes ineffective
10 in VCR as accurate text restoration depends on the combined information from
11 provided images, context, and subtle cues from the tiny exposed areas of masked
12 texts. We develop a pipeline to generate synthetic images for the VCR task using
13 image-caption pairs, with adjustable caption visibility to control the task difficulty.
14 With this pipeline, we construct a dataset for VCR called VCR-WIKI using images
15 with captions from Wikipedia, comprising 2.11M English and 346K Chinese
16 entities in both *easy* and *hard* configurations. Our results reveal that current vision
17 language models significantly lag behind human performance in the VCR task, and
18 merely fine-tuning the models on our dataset does not lead to notable improvements.
19 Solving VCR likely requires complex system-2 level reasoning capability, which
20 existing models struggle with, while humans excel. We release VCR-WIKI and the
21 construction code to promote further research in this area.

22 1 Introduction

23 Recent advances in large language models, such as ChatGPT
24 [39, 38] and Llama [48], have spurred significant interest and
25 progress in the field of vision-language models. With models
26 like GPT-4V [38] and LLaVA [26, 27, 28] blending textual and
27 visual information, the intersection of computer vision and natural
28 language processing has become a vibrant research frontier.
29 These integrated models aim to leverage the potential of vision
30 and language modalities to understand and interpret multimedia
31 content more effectively.

32 Amidst this evolving landscape, we introduce VCR, a novel
33 vision-language task designed to challenge existing models
34 uniquely. VCR challenges these models to restore obscured
35 texts within images, a task that demands an intricate synthesis
36 of text, vision, and text embedded in the image. The VCR task is
37 grounded in two key insights: (1) text embedded within images,
38 with its characteristics different from common visual elements,
39 represents a distinct modality that requires careful alignment of
40 vision, textual data, and the structure of written texts, and (2) neuroscience findings that suggest



Figure 1: An example of the VCR task.

41 that humans are proficient in recognizing partially occluded objects through sophisticated visual and
42 cognitive processes [47, 40, 49, 13, 24]. By leveraging these insights, VCR seeks to explore how
43 well vision-language models can handle texts embedded within images, aligning visual elements and
44 natural language to mimic human-like multimodal understanding and recognition.

45 The Visual Question Answering (VQA) task [3, 51, 35, 43] has been a popular benchmark in assessing
46 how well models align and interpret visual and linguistic information. Traditional VQA approaches,
47 however, predominantly focus on direct queries about visible elements in images and do not address
48 the nuanced relationship between textual content embedded within the image and the overall image
49 context. This gap underscores the limited capabilities of current models in processing integrated
50 visual-textual data, particularly when the textual component, which plays a critical role, is partially
51 obscured or altered.

52 To address these limitations, our VCR task introduces a distinct challenge: restoring occluded text
53 in images. This task taps into system-2 reasoning, which involves complex cognitive processes
54 that go beyond the quick, reflexive responses typical of system-1 reasoning. System-2 reasoning
55 requires deep thinking, logical analysis, and integration of multiple types of information, similar to
56 the capabilities needed to solve the VCR task. Besides, our VCR task builds on the premise that
57 effective text restoration from images requires an integrated understanding beyond the capabilities of
58 current VQA benchmarks. For example, in extreme cases, models rely on existing Optical Character
59 Recognition (OCR) system to extract text from documents [43, 7]. The extracted text is then used as
60 context for generating answers, without a true semantic alignment between the text and the visual
61 elements of the document. This approach, while effective in simple scenarios, falls short in more
62 complex settings where text is intricately woven into the visual narrative of the image.

63 To develop the VCR task, in this work, we introduce a pipeline for generating synthetic images
64 that allows for manipulation of the visibility of the textual components of the image. This not only
65 enhances the challenge posed by the task, but also provides a scalable way to adjust task difficulty.
66 The resulting dataset, VCR-WIKI, comprises 2.11M English data and 346K Chinese data sourced
67 from Wikipedia, featuring captions in both languages across ‘easy’ and ‘hard’ difficulty levels. Our
68 evaluations indicate that existing vision-language models significantly underperform compared to
69 human benchmarks, underscoring the need for novel model architectures and training paradigms
70 specifically geared towards this complex intermodal alignment.

71 By releasing VCR-WIKI and the accompanying dataset construction code, we aim to stimulate
72 further research in this area, encouraging the development of models that can more adeptly navigate
73 the nuanced landscape of the restoration of text embedded in images. This effort aligns with the
74 broader goal of advancing vision-language models to achieve a deeper, more intuitive understanding
75 of multimedia content, bridging the gap between human and machine perception. The code in fully
76 anonymous is available at https://anonymous.4open.science/r/VCR_anonymous/.

77 **Contributions** The main contributions of this paper are:

- 78 **C1** Introduce the VCR task to challenge vision-language models to restore occluded texts in
79 images that need complex System-2 level reasoning.
- 80 **C2** Develop a pipeline for generating synthetic images with embedded text that allows for
81 adjusting visibility of such text, thus providing a rich testing environment for VCR.
- 82 **C3** Create and release VCR-WIKI, a dataset with multilingual captions from Wikipedia images,
83 designed to benchmark vision-language models (VLMs) on text restoration tasks.
- 84 **C4** Conduct empirical evaluations that show significant gaps between current models and
85 human performance on the VCR task. This highlights the effectiveness of VCR for assessing
86 advancements in VLMs, and underscores the necessity for innovative model architectures
87 and training techniques.

88 **2 VCR Task Description**

89 In this section, we compare the VCR task with other existing tasks and aim to answer the following
90 questions:

- 91 **Q1** What is the difference between VCR and other visual reconstruction tasks?

92 **Q2** Why should we care about VCR?

93 For better clarity, we define *text embedded in image (TEI)* as text incorporated within the image.
94 The term *visual image (VI)* pertains to the portion of the image that excludes the text embedded in
95 the image. The *string text (ST)* is not part of the image itself, but is associated with it as a distinct
96 textual element. It is usually the question prompt in the form of natural language, for example,
97 ‘What are the covered texts in the image? Please only guess the covered texts without outputting an
98 explanation.’. Consequently, an element of a VCR task can be expressed as $(ST, (VI, TEI))$, where
99 *ST* is represented as a string and both *VI* and *TEI* are presented in image form. This notation does
100 not imply that *VI* and *TEI* can be physically separated into two distinct image components. Instead,
101 this definition is adopted merely to facilitate a clearer explanation of the concepts involved. Please
102 refer to Figure 3 for an illustration of *VI*, *TEI*, and *ST*.

103 **A1** Existing tasks that are similar to VCR are the tasks of VQA and OCR. VQA takes as input images
104 and a natural language question and generates a free-form response. As the ground-truth response
105 is not unique, evaluating VQA poses a major challenge. In contrast to VQA, OCR is a task where
106 the ground-truth responses are unique: OCR takes as input complete characters in image form and
107 outputs a string representing the characters in the image, without considering the image context.
108 Models pretrained with OCR are able to retrieve texts embedded in the input image, even if they are
109 incomplete or vague. However, as the vagueness or occlusion of the textual components of the image
110 increases, retrieving the original text without considering the remaining nontextual image context
111 becomes harder, and OCR is no longer a good approach. VCR bridges the gap between OCR and
112 VQA: it reconstructs the unique text found in the image while also considering the visual context of
113 the rest of the image.

114 Figure 3 is an example VCR task in hard mode, and Figure 1 shows an example VCR task in the easy
115 mode. Although humans can still fill the blanks easily in the hard mode, it is nearly impossible for
116 models with only OCR capabilities to recover the covered texts without using the context. This is
117 because the pixel-level hints of single characters no longer correspond to a unique solution.

118 **A2** The proposed VCR task is significant in two aspects.

119 The first aspect of importance stems from discoveries in neuroscience about human cognitive abilities
120 to recognize partially occluded objects [13, 24]. Although existing models can recognize objects
121 and texts in images, they often struggle with the complexity of occluded objects due to significant
122 information loss in the images. In contrast, humans excel at filling in missing information using a
123 combination of low-level visual processing and high-level cognitive functions, such as those managed
124 by the prefrontal cortex. This cortical area is known to handle complex cognitive processes such
125 as decision-making and memory retention, which are essential for integrating fragmented visual
126 input into coherent objects. We believe that the occlusion restoration task serves as a probe that can
127 effectively distinguish low-level recognition and high-level cognition involving reasoning. In addition,
128 understanding these neural mechanisms can inspire new algorithms capable of mimicking human-like
129 perception and interpretation in dynamic, real-world conditions where occlusion is common.

130 The second aspect underscores the unique challenge presented by the VCR task, distinguishing
131 it significantly from existing benchmarks, such as traditional VQA or the occluded object
132 restoration task. By occluding texts instead of common visual objects, VCR targets the models’
133 text-image alignment capability, which is one of the major challenges for vision-language models.
134 VCR mandates that models align textual and visual information in a manner that replicates
135 human-like understanding involving the utilization of both textual and visual clues. This
136 task requires a deep integration of visual (*VI*), embedded textual (*TEI*), and contextual inter-
137 pretation across modalities, pushing beyond simple text extraction as performed in OCR tasks. In
138 OCR, the focus is primarily on recognizing visible characters, often without the need to understand
139 their contextual relevance within the image narrative. In contrast, VCR introduces complexity by
140 requiring the model to use available partial texts and the visual context collaboratively to reconstruct
141
142
143
144
145
146
147

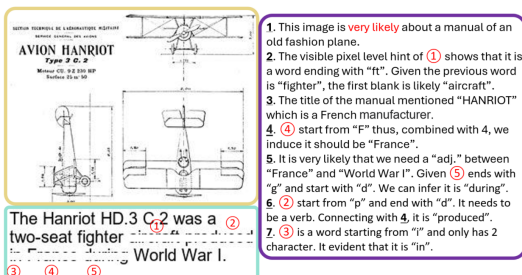


Figure 2: An example of how humans would solve the VCR task.

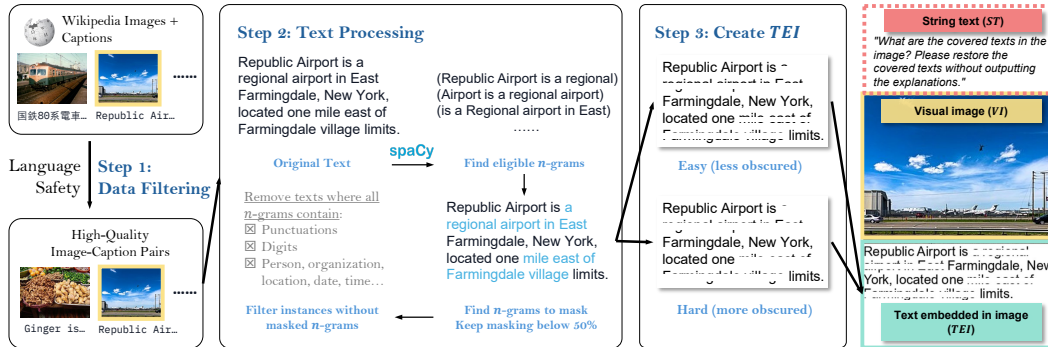


Figure 3: Illustration of the dataset creation pipeline for VCR-WIKI. visual image (VI), text embedded in image (TEI) and string text (ST) in an example of the English Hard configuration of VCR-WIKI. The solid line-enclosed contents (VI and TEI) are part of the image, whereas the dotted line-enclosed content (ST) is given separately from the image.

148 the obscured content accurately. This not only tests the model’s ability to process *TEI-VI* modalities
 149 effectively, but also challenges it to maintain internal consistency and System-2 level reasoning skill,
 150 akin to human cognitive processes where context and visual clues guide understanding and response.
 151 Below we show an example of how humans would solve this task in ‘hard’ difficulty in Figure 2.

152 3 Dataset Creation

153 The VCR task aligns visual images (VI) with text embedded in images (ET) by using highly correlated
 154 image-text pairs. We create VCR-WIKI, a Wikipedia-based VCR dataset, using images and captions
 155 from Wikipedia¹, filtering out sensitive content such as NSFW and crime-related terms. Each instance
 156 includes a stacked VI+ET image and a question-answer pair, mimicking a VQA format. The VI+ET
 157 images are resized to 300 pixels wide, with ET truncated to five lines to avoid excessive height. We
 158 exclude instances where VI+ET exceeds 900 pixels in height.

159 For masking within ET, we randomly select 5-grams using spaCy, excluding terms like numbers,
 160 names, locations, etc. The 5-grams are partially obscured to vary task difficulty, but the total masked
 161 tokens don’t exceed 50% of the caption. Images without an eligible 5-gram are excluded. An ablation
 162 version retains only the ET portion to assess the impact of VI on model performance.

163 The task involves a question prompting the model to restore the obscured text, with ground truth
 164 corresponding to the visible caption. The dataset supports both English and Chinese, offering two
 165 difficulty levels: an easy version where OCR models fail but native speakers succeed, and a hard
 166 version with minimal visible text. The dataset is released under CC BY-SA 4.0 but is not linked due
 167 to anonymity. Please refer to Appendix C for more details.

168 4 Experiments

169 In this section, we report the experiment results of existing state-of-the-art vision-language models
 170 on our proposed VCR tasks. The fine-tuning and evaluation of open-source models are conducted on
 171 a mix of NVIDIA A100 80G and L40S 48G GPUs in an internal cluster.

172 4.1 Models

173 **Closed-source Models.** We evaluate several most advanced proprietary models with their provided
 174 APIs. The evaluated models include GPT-4o (gpt-4o-2024-0513), GPT-4 Turbo (gpt-4-turbo-2024-
 175 04-09), GPT-4V (gpt-4-1106-vision-preview) [39, 38], Claude 3 Opus (claude-3-opus-20240229),
 176 Claude 3.5 Sonnet (claude-3-5-sonnet-20240620) [2], Gemini 1.5 pro (gemini-1.5-pro-001) [45],
 177 Reka Core (reka-core-20240501) [46], and Qwen-VL-Max (tested on May 2024) [4].

¹Datasource: https://huggingface.co/datasets/wikimedia/wit_base.

178 **Open-source Models.** We evaluate open-source models with the best performance on the
 179 OpenVLM Leaderboard² and state-of-the-art Chinese VLM models. The evaluated models in-
 180 clude InternVL-Chat-V1.5[10], MiniCPM-Llama3-V2.5 [18], InternLM-XComposer2-VL-7B [12],
 181 CogVLM2-Llama3-19B-Chat [52], Idefics2-8B [23], Yi-VL-34B [1], Yi-VL-6B [1], Qwen-VL-
 182 Chat [4], DeepSeek-VL-7B-Chat [30], DeepSeek-VL-1.3B-Chat [30], Monkey [29, 25] and DocOwl-
 183 1.5 [15]. Out of these models, Idefics2-8B is an English-only model, and CogVLM2-Llama3-19B-
 184 Chat has its Chinese variant, CogVLM2-Llama3-19B-Chinese-Chat. Please refer to Table 6 for the
 185 model specifications.

186 **Finetuned Models.** To test whether VLMs can learn to conduct VCR via fine-tuning, we select two
 187 models from the open-sourced models, CogVLM2-Llama3-19B-Chat and MiniCPM-Llama3-V2.5,
 188 and fine-tune them on a subset of VCR’s training set.

189 More specifically, we fine-tune CogVLM2-Llama3-19B-Chat and MiniCPM-Llama3-V2.5 in the
 190 English Hard configuration, and CogVLM2-Llama3-19B-Chinese-Chat and MiniCPM-Llama3-V2.5
 191 on the Chinese Hard configuration. The models are finetuned using LoRA [16] with $r = 8$ and
 192 $\alpha = 32$. We adopt the schedule-free AdamW optimizer [11] with a learning rate $2e - 4$. The effective
 193 batch size is 64. Each model is trained on the first 16,000 examples of the training set for 1 epoch.
 194 All fine-tuning experiments are performed on a single node with 4 NVIDIA L40S 48G GPUs.

195 4.2 Metrics

196 We measure the quality of the model’s restoration of each masked n -gram (where $n = 5$ in our
 197 setting, as specified in Section C). Due to the variability of different models’ outputs, for each masked
 198 n -gram $m \in \mathbb{V}_e^n$, where \mathbb{V}_e is the vocabulary of the evaluation tokenizer³, we extract the most similar
 199 n -gram $\hat{m} \in \mathbb{V}_e^n$ with the least edit distance in the model’s generation.

200 We report the two metrics below in our experiment section to measure the restoration quality: **Exact**
 201 **Match** (EM), which measures whether the restored n -gram \hat{m} totally matches the ground-truth m ;
 202 and **Jaccard Index** (J), which measures the similarity of \hat{m} and m as bag-of-words.

203 • **Exact Match** (EM), which measures whether the restored n -gram \hat{m} totally matches the
 204 ground-truth m ;

$$EM(m, \hat{m}) = \begin{cases} 1 & \text{if } m = \hat{m}, \\ 0 & \text{otherwise} \end{cases}.$$

205 • **Jaccard Index** (J), which is a more relaxed metric that measures the similarity of \hat{m} and m
 206 as bag-of-words.

$$J(m, \hat{m}) = \frac{|S(m) \cap S(\hat{m})|}{|S(m) \cup S(\hat{m})|},$$

207 where $S(m)$ represents the set of tokens in m .

208 4.3 Experimental Results

209 Please refer to the exact match score and the Jaccard-index of the evaluation in Table 2.

210 **Open-Source Models.** We evaluate each open-source model based on the whole 5,000 examples in
 211 the test set. Note that Idefics2-8B only supports the English task, hence it has no evaluation score on
 212 the Chinese task.

213 Although achieving state-of-the-art performance on the Open VLM leaderboard, almost all the
 214 tested models achieve a low exact match accuracy in the English Easy configuration and fail on
 215 the other settings. The best open-source model across the 4 configurations (English Easy, English
 216 Hard, Chinese Easy, and Chinese Hard) is CogVLM2-Llama3-Chat. This might be attributed to

²We selected the highest-performing open-source models with fewer than 40 billion parameters from the OpenVLM Leaderboard as of May 23, 2024. Details are available at https://huggingface.co/spaces/opencompass/open_vlm_leaderboard.

³We utilize spaCy’s `en_core_web_sm`’s and `zh_core_web_sm`’s tokenizer for English and Chinese evaluation, respectively.

217 its pretraining process and the special architecture. We also notice that VI has a negative impact
 218 for most models on the exact match scores ($\Delta < 0$), which means that the image information is
 219 not properly utilized. The best performed open-source model on average, CogVLM2-Llama3-Chat
 220 and CogVLM2-Llama3-Chinese-Chat, and its fine-tuned version have positive Δ , except for the
 221 Chinese Hard configuration. This indicates that information from VI could help improve the model
 222 performance on VCR.

223 For different languages, we noticed a large performance drop when testing the model in Chinese
 224 configurations, despite the fact that all models claim to have basic English-Chinese duolingual
 225 capabilities. This is somehow surprising, since Chinese characters, due to their logographic nature,
 226 may exhibit a higher degree of recognizability compared to languages that use alphabetic scripts in
 227 one order [54, 62].

228 Moreover, we found that models, such as internlm-xcomposer2, are good at OCR and understanding
 229 image documents (as demonstrated by DocOwl 1.5 and Monkey) still have the potential to be
 230 improved in the VCR task. This highlights the unique and indispensable role of VCR in the current
 231 suite of benchmarks. Excelling in other document-related benchmarks does not guarantee similar
 232 performance in VCR tasks, emphasizing VCR’s distinct challenges and value.

233 **Closed-Source Models.** We evaluate every closed-source model with the first 500 examples in the
 234 test set. In English tasks, GPT-4o scores the best among the models that have not been finetuned.
 235 Even though GPT-4 series support Chinese, we found that GPT-4V (gpt-4-1106-vision-preview) is
 236 not able to recognize Chinese characters embedded in the image even without any occlusion. Thus,
 237 we do not test GPT-4V on Chinese tasks.

238 In English configurations, closed-source models outperform all open-source models except
 239 CogVLM2, which indicates that model scaling might help improve performance on the VCR task.
 240 However, compared with the human evaluation results in Section 4.4, we notice a large performance
 241 gap, especially in the English Hard configuration. This shows significant room for improvement in
 242 the current state-of-the-art models.

243 Please refer to Table 4 to compare open and closed source models using the same 500 test cases.

244 **4.4 Human Evaluation**

245 We recruited 7 volunteers to perform human evaluation on a subset of the samples of our datasets.
 246 Two out of the seven evaluators are native English speakers, while five are native Chinese speakers
 247 who are also fluent in English⁴. All volunteers have earned postgraduate degrees majoring in one
 248 of the following fields: biology, statistics, computer science, and economics. The evaluations were
 249 conducted on a voluntary basis and participants received no rewards.

250 We gave the volunteer the following instructions: (1) We ask the volunteers to focus on the puzzles.
 251 Each example in the hard collection may require 30 seconds to 2 minutes of focused attention; and
 252 (2) we ask the volunteers to utilize the context rather than directly brute-force the puzzle.

253 Every sample is solved by at least 3 volunteers. In English, we release the exact match score in 2
 254 splits: all errors counted (All), and only count errors not related to date and person names (Filtered).

Table 1: Human evaluation results on the VCR task for in terms of exact matches. N is the number of puzzles in each language.

	EN Easy (N = 169)		EN Hard (N = 169)		ZH Easy (N = 188)		ZH Hard (N = 188)	
	Mean (%)	SD (%)	Mean (%)	SD (%)	Mean (%)	SD (%)	Mean (%)	SD (%)
All	96.65	0.34	91.12	1.18	98.58	0.31	91.84	0.81
Filtered	98.62	0.34	97.63	2.13	99.47	0.00	96.63	1.11

255 Refer to Table 3 to compare all models with human evaluation results using the same test cases.

⁴The TOEFL scores of the non-native English-speaking participants range from 102/120 to 112/120.

Table 2: Performance of vision language models on VCR task in English (EN) and Chinese (ZH), for easy and hard modes. FT indicates finetuning on 16,000 VCR-wiki samples. Best results: underlined (finetuned), bold (non-finetuned). Subscripts show bootstrap standard deviation.

Language	Mode	Open/closed source	Model name	Model size	Exact match (%) \uparrow			Jaccard index (%) \uparrow		
					VI + TEI	TEI	Δ	VI + TEI	TEI	Δ
English	Easy	Closed	Claude 3 Opus	-	62.0 _{0.13}	77.0 _{0.5}	-15	77.67 _{0.32}	88.41 _{0.39}	-10.74
			Claude 3.5 Sonnet	-	63.85 _{1.71}	72.81 _{1.56}	-8.94	74.65 _{1.33}	83.48 _{1.14}	-8.83
			Gemini 1.5 Pro	-	62.73 _{1.66}	82.98 _{1.3}	-20.25	77.71 _{1.21}	91.56 _{0.76}	-13.85
			GPT-4 Turbo	-	78.74 _{0.13}	81.94 _{0.25}	-3.2	88.54 _{0.24}	92.18 _{0.3}	-3.65
			GPT-4o	-	91.55_{0.29}	94.56_{0.13}	-3.01	96.44_{0.11}	97.76_{0.06}	-1.32
			GPT-4V	-	52.04 _{0.24}	37.86 _{0.22}	14.17	65.36 _{0.39}	54.13 _{0.41}	11.23
			Qwen-VL-Max	-	76.8 _{0.5}	85.53 _{0.19}	-8.74	85.71 _{0.28}	91.45 _{0.29}	-5.74
			Reka Core	-	66.46 _{1.64}	78.51 _{1.42}	-12.05	84.23 _{0.86}	90.45 _{0.7}	-6.22
			Cambrian-1	34B	79.69 _{0.43}	81.28 _{0.43}	-1.59	89.27 _{0.28}	92.54 _{0.19}	-3.27
			CogVLM2	19B	83.25 _{0.07}	78.29 _{0.04}	4.96	89.75 _{0.1}	88.07 _{0.08}	1.68
			CogVLM2-FT	19B	<u>93.27_{0.03}</u>	<u>92.63_{0.07}</u>	0.64	<u>97.62_{0.02}</u>	<u>97.46_{0.01}</u>	0.22
			DeepSeek-VL	1.3B	23.04 _{0.05}	31.09 _{0.12}	-8.04	46.84 _{0.07}	52.36 _{0.06}	-5.52
		DeepSeek-VL	7B	38.01 _{0.12}	45.94 _{0.1}	-7.93	60.02 _{0.15}	64.72 _{0.04}	-4.7	
		DocOwl-1.5-Omni	8B	0.84 _{0.01}	1.55 _{0.02}	-0.71	13.34 _{0.03}	14.62 _{0.04}	-1.28	
		Monkey	7B	50.66 _{0.1}	56.2 _{0.08}	-5.54	67.6 _{0.09}	72.82 _{0.08}	-5.22	
		Idedics2	8B	15.75 _{0.11}	27.77 _{0.11}	-12.02	31.97 _{0.02}	51.0 _{0.03}	-19.03	
		InternLM-XComposer2-VL	7B	46.64 _{0.1}	46.4 _{0.11}	0.24	70.99 _{0.1}	72.14 _{0.07}	-1.14	
		InternLM-XComposer2.5-VL	7B	41.35 _{0.55}	25.37 _{0.51}	15.97	63.04 _{0.42}	49.95 _{0.41}	13.09	
		InternVL-V1.5	25.5B	14.65 _{0.13}	75.06 _{0.1}	-60.41	51.42 _{0.04}	87.1 _{0.03}	-35.68	
		InternVL-V2	25.5B	74.51 _{0.48}	77.79 _{0.47}	-3.27	86.74 _{0.28}	89.02 _{0.26}	-2.28	
		InternVL-V2	40B	84.67_{0.40}	87.71_{0.37}	-3.04	92.64_{0.22}	95.10_{0.16}	-2.47	
		MiniCPM-V2.5	8B	31.81 _{0.08}	40.05 _{0.09}	-8.25	53.24 _{0.1}	63.2 _{0.1}	-9.96	
		MiniCPM-V2.5-FT	8B	40.96 _{0.08}	44.62 _{0.08}	-3.67	64.4 _{0.05}	67.62 _{0.1}	-3.22	
		Qwen-VL	7B	49.71 _{0.17}	52.15 _{0.15}	-2.44	69.94 _{0.07}	72.28 _{0.08}	-2.34	
	Yi-VL	34B	0.82 _{0.03}	1.61 _{0.04}	-0.79	5.59 _{0.04}	7.72 _{0.03}	-2.13		
	Yi-VL	6B	0.75 _{0.01}	1.65 _{0.01}	-0.9	5.54 _{0.02}	7.76 _{0.03}	-2.22		
	Hard	Closed	Claude 3 Opus	-	37.8 _{0.28}	50.0 _{0.33}	-12.2	57.68 _{0.8}	70.16 _{0.64}	-12.48
			Claude 3.5 Sonnet	-	41.71 _{1.69}	44.72 _{1.78}	-2.98	56.15 _{1.46}	58.54 _{1.6}	-2.4
			Gemini 1.5 Pro	-	28.07 _{1.58}	38.76 _{1.68}	-10.68	51.91 _{1.22}	59.62 _{1.27}	-7.72
			GPT-4 Turbo	-	45.15 _{0.28}	48.64 _{0.57}	-3.5	65.72 _{0.25}	67.86 _{0.2}	-2.14
			GPT-4o	-	73.2_{0.16}	82.43_{0.17}	-9.22	86.17_{0.21}	92.01_{0.2}	-5.84
			GPT-4V	-	25.83 _{0.44}	14.95 _{0.3}	10.87	44.63 _{0.48}	30.08 _{0.67}	14.56
			Qwen-VL-Max	-	41.65 _{0.32}	52.72 _{0.2}	-11.07	61.18 _{0.35}	70.19 _{0.37}	-9.01
			Reka Core	-	6.71 _{0.89}	11.81 _{1.15}	-4.47	25.84 _{0.95}	35.83 _{1.05}	-9.99
			Cambrian-1	34B	27.20 _{0.48}	29.68_{0.50}	-2.48	50.04 _{0.40}	55.66_{0.39}	-5.62
			CogVLM2	19B	37.98_{0.18}	17.68 _{0.06}	20.3	59.99_{0.05}	39.69 _{0.03}	20.3
			CogVLM2-FT	19B	<u>77.44_{0.05}</u>	<u>66.07_{0.13}</u>	11.38	<u>90.17_{0.03}</u>	<u>83.41_{0.07}</u>	6.76
			DeepSeek-VL	1.3B	0.16 _{0.01}	0.39 _{0.02}	-0.23	11.89 _{0.02}	11.47 _{0.03}	0.42
		DeepSeek-VL	7B	1.0 _{0.02}	1.75 _{0.03}	-0.75	15.9 _{0.08}	17.2 _{0.04}	-1.3	
		DocOwl-1.5-Omni	8B	0.04 _{0.0}	0.02 _{0.0}	0.01	7.76 _{0.01}	7.74 _{0.02}	0.03	
		Monkey	7B	1.99 _{0.04}	2.43 _{0.03}	-0.48	14.02 _{0.03}	14.11 _{0.03}	-0.09	
		Idedics2	8B	0.65 _{0.01}	0.94 _{0.02}	-0.29	9.95 _{0.05}	12.57 _{0.02}	-2.64	
		InternLM-XComposer2-VL	7B	0.7 _{0.01}	0.92 _{0.01}	-0.22	12.51 _{0.02}	13.23 _{0.02}	-0.72	
		InternLM-XComposer2.5-VL	7B	0.93 _{0.11}	1.11 _{0.11}	-0.18	13.82 _{0.16}	14.72 _{0.18}	-0.89	
		InternVL-V1.5	25.5B	1.99 _{0.02}	6.49 _{0.04}	-4.5	16.73 _{0.06}	26.4 _{0.03}	-9.67	
		InternVL-V2	25.5B	6.18 _{0.27}	6.38 _{0.27}	-0.20	24.52 _{0.29}	24.37 _{0.30}	0.16	
		InternVL-V2	40B	13.10 _{0.37}	19.16 _{0.44}	-6.06	33.64 _{0.36}	41.35 _{0.39}	-7.71	
		MiniCPM-V2.5	8B	1.41 _{0.03}	1.96 _{0.02}	-0.55	11.94 _{0.02}	13.37 _{0.04}	-1.43	
MiniCPM-V2.5-FT		8B	13.86 _{0.1}	13.73 _{0.05}	0.12	36.89 _{0.06}	36.51 _{0.06}	0.38		
Qwen-VL		7B	2.0 _{0.03}	2.32 _{0.03}	-0.32	15.04 _{0.05}	14.27 _{0.05}	0.77		
Yi-VL	34B	0.07 _{0.0}	0.05 _{0.0}	0.02	4.31 _{0.02}	5.89 _{0.02}	-1.58			
Yi-VL	6B	0.06 _{0.0}	0.04 _{0.0}	0.02	4.46 _{0.02}	5.91 _{0.01}	-1.46			
Chinese	Easy	Closed	Claude 3 Opus	-	0.9 _{0.3}	1.0 _{0.31}	-0.1	11.5 _{0.48}	10.0 _{0.49}	1.49
			Claude 3.5 Sonnet	-	1.0 _{0.31}	0.8 _{0.28}	0.2	7.5 _{0.54}	7.5 _{0.51}	0.03
			Gemini 1.5 Pro	-	1.1 _{0.32}	0.7 _{0.22}	0.6	11.1 _{0.56}	11.47 _{0.48}	-0.37
			GPT-4o	-	14.87_{1.14}	22.48_{1.35}	-7.58	39.05_{0.99}	48.24_{1.09}	-9.19
			GPT-4 Turbo	-	0.21 _{0.14}	0.1 _{0.1}	0.1	8.4 _{0.56}	6.97 _{0.29}	1.45
			Qwen-VL-Max	-	6.34 _{0.08}	9.92 _{0.09}	-3.58	13.45 _{0.41}	22.86 _{0.46}	-9.42
			Reka Core	-	0.0 _{0.0}	0.0 _{0.0}	0	3.43 _{0.26}	3.15 _{0.2}	0.28
			CogVLM2-Chinese	19B	33.24_{0.04}	30.7_{0.07}	2.54	57.57_{0.06}	53.66_{0.04}	3.91
			CogVLM2-Chinese-FT	19B	<u>61.69_{0.05}</u>	<u>59.85_{0.08}</u>	1.84	<u>78.14_{0.05}</u>	<u>77.12_{0.03}</u>	1.02
			DeepSeek-VL	1.3B	0.0 _{0.0}	0.0 _{0.0}	0	6.56 _{0.01}	3.17 _{0.02}	3.4
			DeepSeek-VL	7B	0.0 _{0.0}	0.0 _{0.0}	0	4.08 _{0.01}	6.84 _{0.01}	-2.76
			DocOwl-1.5-Omni	8B	0.0 _{0.0}	0.0 _{0.0}	0	1.14 _{0.01}	3.38 _{0.01}	-2.23
		Monkey	7B	0.62 _{0.01}	1.44 _{0.01}	-0.82	8.34 _{0.06}	10.95 _{0.03}	-2.61	
		InternLM-XComposer2-VL	7B	0.27 _{0.01}	0.23 _{0.01}	0.04	12.32 _{0.02}	12.28 _{0.03}	0.04	
		InternLM-XComposer2.5-VL	7B	0.46 _{0.07}	0.58 _{0.08}	-0.12	12.97 _{0.16}	14.99 _{0.17}	-2.01	
		InternVL-V1.5	25.5B	4.78 _{0.02}	5.32 _{0.02}	-0.55	26.43 _{0.03}	21.7 _{0.04}	4.72	
		InternVL-V2	25.5B	9.02 _{0.28}	7.92 _{0.26}	1.10	32.30 _{0.29}	26.90 _{0.28}	5.60	
		InternVL-V2	40B	22.09 _{0.41}	17.26 _{0.39}	4.84	47.62 _{0.34}	37.93 _{0.35}	9.69	
		MiniCPM-V2.5	8B	4.1 _{0.02}	5.05 _{0.08}	-0.95	18.03 _{0.07}	22.94 _{0.04}	-4.9	
		MiniCPM-V2.5-FT	8B	7.4 _{0.33}	7.92 _{0.03}	-0.49	29.87 _{0.04}	31.32 _{0.03}	-1.45	
		Qwen-VL	7B	0.04 _{0.01}	0.0 _{0.0}	0.04	1.5 _{0.01}	0.34 _{0.01}	1.15	
		Yi-VL	34B	0.0 _{0.0}	0.0 _{0.0}	0	4.44 _{0.01}	1.8 _{0.01}	2.64	
		Yi-VL	6B	0.0 _{0.0}	0.0 _{0.0}	0	4.37 _{0.01}	1.76 _{0.0}	2.6	
		Hard	Closed	Claude 3 Opus	-	0.5 _{0.18}	0.1 _{0.1}	0.2	9.22 _{0.38}	8.09 _{0.33}
	Claude 3.5 Sonnet			-	0.2 _{0.15}	0.0 _{0.0}	0.2	4.0 _{0.3}	2.47 _{0.23}	1.63
	Gemini 1.5 Pro			-	0.7 _{0.26}	0.5 _{0.23}	0.2	11.82 _{0.51}	11.75 _{0.44}	0.07
	GPT-4o			-	2.2_{0.47}	1.8_{0.4}	0.4	22.72_{0.67}	22.89_{0.65}	-0.17
	GPT-4 Turbo			-	0.0 _{0.0}	0.2 _{0.13}	-0.2	8.58 _{0.3}	6.87 _{0.28}	1.72
	Qwen-VL-Max			-	0.89 _{0.06}	1.38 _{0.1}	-0.49	5.4 _{0.19}	12.29 _{0.18}	-6.89
	Reka Core			-	0.0 _{0.0}	0.0 _{0.0}	0	3.35 _{0.23}	2.97 _{0.2}	0.38
	CogVLM2-Chinese			19B	1.34_{0.03}	2.67_{0.02}	-1.32	17.35_{0.03}	19.51_{0.03}	-2.16
	CogVLM2-Chinese-FT			19B	<u>42.11_{0.09}</u>	<u>45.63_{0.06}</u>	-3.51	<u>65.67_{0.15}</u>	<u>69.28_{0.04}</u>	-3.61
	DeepSeek-VL			1.3B	0.0 _{0.0}	0.0 _{0.0}	0	6.46 _{0.01}	3.22 _{0.02}	3.24
	DeepSeek-VL			7B	0.0 _{0.0}	0.0 _{0.0}	0	5.11 _{0.01}	7.21 _{0.01}	-2.1
	DocOwl-1.5-Omni			8B	0.0 _{0.0}	0.0 _{0.0}	0	1.37 _{0.01}	4.07 _{0.02}	-2.7
	Monkey		7B	0.12 _{0.01}	0.07 _{0.0}	0.05	6.36 _{0.01}	6.68 _{0.03}	-0.32	
	InternLM-XComposer2-VL		7B	0.07 _{0.01}	0.09 _{0.0}	-0.02	8.97 _{0.02}	8.51 _{0.01}	0.46	
	InternLM-XComposer2.5-VL		7B	0.11 _{0.04}	0.12 _{0.01}	-0.01	10.95 _{0.11}	11.43 _{0.12}	-0.48	
	InternVL-V1.5		25.5B	0.03 _{0.0}	0.1 _{0.01}	-0.07	8.46 _{0.01}	6.27 _{0.04}	2.19	
	InternVL-V2		25.5B	0.05 _{0.02}	0.22 _{0.05}	-0.18	9.49 _{0.10}	9.90 _{0.12}	-0.41	
	InternVL-V2		40B	0.48 _{0.07}	0.74 _{0.08}	-0.26	12.57 _{0.14}	13.31 _{0.15}	-0.74	
	MiniCPM-V2.5		8B	0.09 _{0.0}	0.08 _{0.0}	0.01	7.39 _{0.02}	7.89 _{0.01}	-0.5	
	MiniCPM-V2.5-FT		8B	1.53 _{0.01}	1.11 _{0.02}	0.42	18.0 _{0.03}	15.35 _{0.02}	2.65	
	Qwen-VL		7B	0.01 _{0.0}	0.01 _{0.0}	0	1.17 _{0.01}	0.12 _{0.0}		

256 5 Related Work

257 **Complex Reasoning in Vision Language Models.** In the emerging field of complex reasoning in
258 vision-language models, several significant contributions have been made to enhance multimodal
259 reasoning capabilities. The Visual CoT dataset [42] is a noteworthy development, introducing a
260 comprehensive dataset for chain-of-thought reasoning across visual contexts, aiming to improve
261 interpretability and precision in multimodal large language models (MLLMs) by annotating key
262 regions in images that inform VQA processes. Similarly, the Zhang et al. [61] extends the chain-
263 of-thought framework to incorporate both visual and textual data, demonstrating improvements
264 in reasoning and inference accuracy on complex multimodal datasets. Further, the benchmark
265 MathVista [31] is put forward as a challenge of mathematical reasoning in visual contexts by
266 evaluating large models on tasks that require both deep visual understanding and mathematical
267 computation, marking a significant step towards models performing complex, real-world tasks.

268 **Visual Question Answering (VQA) and Optical Character Recognition (OCR).** Visual Question
269 Answering (VQA) involves datasets designed for answering questions based on images, such as FVQA
270 [51] and OK-VQA [32], which require external knowledge. CLEVR [21] focuses on visual reasoning,
271 while Text-VQA [43, 6, 36, 53] targets understanding embedded text in images. Various datasets
272 support the Text-VQA task, including TextVQA [43], ST-VQA [6], OCR-VQA [35], InfographicVQA
273 [33], and DocVQA [34]. Optical Character Recognition (OCR) [37] has been widely studied,
274 though classical methods struggle with unconstrained images. Advances in scene-text recognition
275 [5, 14, 19, 20] have improved OCR in the wild, and OCR is integral to Text-VQA tasks. Models
276 like LoRRA [43] and TAP [57] enhance VQA performance by integrating OCR to improve text
277 recognition in images.

278 **Vision Language Model.** Vision-language models are designed for tasks that involve understanding
279 and generating content from images and text [44, 28, 22, 23]. For example, models have been devel-
280 oped to combine Llama3 with advanced vision-language processing capabilities to handle complex
281 multimodal tasks [59, 56, 17, 58, 52, 12]. Qwen-VL [4] enhances visual-linguistic representations
282 for more accurate contextual interpretations, while OpenGVLab-InternVL-Chat [10, 9] merges the
283 InternVL framework with interactive chat capabilities. These studies typically employ a multimodal
284 encoder [41, 60, 55] to process multimodal data, which is then mapped to the same input space
285 of the language model. General-purpose models such as the GPT-4 series models [39, 38], the
286 Claude series models [2], the Gemini series models [45] and the Reka series models [46] have
287 also been adapted for vision-language tasks, demonstrating strong performance in multimodal tasks.
288 Finally, DocLLM [50] specializes in document understanding by integrating visual and textual data
289 to enhance the interpretation and generation of document-related content. These models collectively
290 represent significant advancements in vision-language integration, contributing unique capabilities
291 and enhancements to the understanding and generation of multimodal information.

292 6 Conclusion

293 In this work, we introduced the VCR task, a novel vision-language challenge aimed at promoting the
294 integration of visual and textual modalities, including text embedded in both natural language tokens
295 and image formats and highly obscured text embedded in the image. We developed a specialized
296 pipeline to create a dataset tailored to this task, utilizing correlated image-text pairs. This task stands
297 out from existing methods by requiring a more profound integration of visual cues and partially
298 obscured text, highlighting its uniqueness and importance in the field.

299 We conducted extensive evaluations of state-of-the-art vision-language models (VLMs) in both
300 English and Chinese. The results demonstrated significant room for improvement, suggesting that
301 current models have not yet fully exploited the capabilities necessary for VCR. We selected models
302 representing both the highest and average performance tiers for additional fine-tuning with our dataset.
303 Although fine-tuning exhibited potential for enhancing VCR capabilities, it did not consistently result
304 in significant improvements, indicating the complexity and challenges of adapting models to this task.

305 By introducing the VCR task and its specialized dataset, we aim to advance research in vision-
306 language interaction. The unique challenges of VCR seek to improve model development and
307 training, extending the limits of multimodal AI. We invite the community to utilize our dataset and
308 develop innovative strategies to boost the performance of vision-language models.

309 **References**

- 310 [1] 01.AI, Alex Young, Bei Chen, Chao Li, Chengen Huang, Ge Zhang, Guanwei Zhang, Heng
311 Li, Jiangcheng Zhu, Jianqun Chen, Jing Chang, Kaidong Yu, Peng Liu, Qiang Liu, Shawn
312 Yue, Senbin Yang, Shiming Yang, Tao Yu, Wen Xie, Wenhao Huang, Xiaohui Hu, Xiaoyi
313 Ren, Xinyao Niu, Pengcheng Nie, Yuchi Xu, Yudong Liu, Yue Wang, Yuxuan Cai, Zhenyu Gu,
314 Zhiyuan Liu, and Zonghong Dai. Yi: Open foundation models by 01.ai, 2024.
- 315 [2] Anthropic. The claude 3 model family: Opus, sonnet, haiku. 2024.
- 316 [3] Stanislaw Antol, Aishwarya Agrawal, Jiaseen Lu, Margaret Mitchell, Dhruv Batra, C. Lawrence
317 Zitnick, and Devi Parikh. VQA: Visual Question Answering. In *International Conference on*
318 *Computer Vision (ICCV)*, 2015.
- 319 [4] Jinze Bai, Shuai Bai, Shusheng Yang, Shijie Wang, Sinan Tan, Peng Wang, Junyang Lin, Chang
320 Zhou, and Jingren Zhou. Qwen-vl: A versatile vision-language model for understanding,
321 localization, text reading, and beyond. *arXiv preprint arXiv: 2308.12966*, 2023.
- 322 [5] Alessandro Bissacco, Mark Cummins, Yuval Netzer, and Hartmut Neven. Photoocr: Reading
323 text in uncontrolled conditions. In *Proceedings of the IEEE International Conference on*
324 *Computer Vision (ICCV)*, December 2013.
- 325 [6] Ali Furkan Biten, Ruben Tito, Andres Mafla, Lluís Gomez, Marçal Rusinol, Ernest Valveny,
326 C.V. Jawahar, and Dimosthenis Karatzas. Scene text visual question answering. In *Proceedings*
327 *of the IEEE/CVF International Conference on Computer Vision (ICCV)*, October 2019.
- 328 [7] Fedor Borisjuk, Albert Gordo, and Viswanath Sivakumar. Rosetta: Large scale system for text
329 detection and recognition in images. In *Proceedings of the 24th ACM SIGKDD International*
330 *Conference on Knowledge Discovery & Data Mining, KDD '18*, page 71–79, New York, NY,
331 USA, 2018. Association for Computing Machinery.
- 332 [8] Qiguang Chen, Libo Qin, Jin Zhang, Zhi Chen, Xiao Xu, and Wanxiang Che. M³cot: A novel
333 benchmark for multi-domain multi-step multi-modal chain-of-thought. *arXiv preprint arXiv:*
334 *2405.16473*, 2024.
- 335 [9] Zhe Chen, Weiyun Wang, Hao Tian, Shenglong Ye, Zhangwei Gao, Erfei Cui, Wenwen Tong,
336 Kongzhi Hu, Jiapeng Luo, Zheng Ma, et al. How far are we to gpt-4v? closing the gap to
337 commercial multimodal models with open-source suites. *arXiv preprint arXiv:2404.16821*,
338 2024.
- 339 [10] Zhe Chen, Jiannan Wu, Wenhai Wang, Weijie Su, Guo Chen, Sen Xing, Muyan Zhong, Qinglong
340 Zhang, Xizhou Zhu, Lewei Lu, Bin Li, Ping Luo, Tong Lu, Yu Qiao, and Jifeng Dai. Internvl:
341 Scaling up vision foundation models and aligning for generic visual-linguistic tasks. *arXiv*
342 *preprint arXiv:2312.14238*, 2023.
- 343 [11] Aaron Defazio, Xingyu Yang, Harsh Mehta, Konstantin Mishchenko, Ahmed Khaled, and
344 Ashok Cutkosky. The road less scheduled, 2024.
- 345 [12] Xiaoyi Dong, Pan Zhang, Yuhang Zang, Yuhang Cao, Bin Wang, Linke Ouyang, Xilin Wei,
346 Songyang Zhang, Haodong Duan, Maosong Cao, Wenwei Zhang, Yining Li, Hang Yan, Yang
347 Gao, Xinyue Zhang, Wei Li, Jingwen Li, Kai Chen, Conghui He, Xingcheng Zhang, Yu Qiao,
348 Dahua Lin, and Jiaqi Wang. Internlm-xcomposer2: Mastering free-form text-image composition
349 and comprehension in vision-language large model. *arXiv preprint arXiv: 2401.16420*, 2024.
- 350 [13] Amber M Fyall, Yasmine El-Shamayleh, Hannah Choi, Eric Shea-Brown, and Anitha Pasupathy.
351 Dynamic representation of partially occluded objects in primate prefrontal and visual cortex.
352 *eLife*, 6:e25784, September 2017.
- 353 [14] Ankush Gupta, Andrea Vedaldi, and Andrew Zisserman. Synthetic data for text localisation
354 in natural images. In *Proceedings of the IEEE Conference on Computer Vision and Pattern*
355 *Recognition (CVPR)*, June 2016.

- 356 [15] Anwen Hu, Haiyang Xu, Jiabo Ye, Ming Yan, Liang Zhang, Bo Zhang, Chen Li, Ji Zhang, Qin
357 Jin, Fei Huang, and Jingren Zhou. mplug-docowl 1.5: Unified structure learning for ocr-free
358 document understanding. *arXiv preprint arXiv: 2403.12895*, 2024.
- 359 [16] Edward J Hu, yelong shen, Phillip Wallis, Zeyuan Allen-Zhu, Yuanzhi Li, Shean Wang,
360 Lu Wang, and Weizhu Chen. LoRA: Low-rank adaptation of large language models. In
361 *International Conference on Learning Representations*, 2022.
- 362 [17] Jinyi Hu, Yuan Yao, Chongyi Wang, Shan Wang, Yinxu Pan, Qianyu Chen, Tianyu Yu, Hanghao
363 Wu, Yue Zhao, Haoye Zhang, Xu Han, Yankai Lin, Jiao Xue, Dahai Li, Zhiyuan Liu, and
364 Maosong Sun. Large multilingual models pivot zero-shot multimodal learning across languages.
365 *arXiv preprint arXiv:2308.12038*, 2023.
- 366 [18] Shengding Hu, Yuge Tu, Xu Han, Chaoqun He, Ganqu Cui, Xiang Long, Zhi Zheng, Yewei
367 Fang, Yuxiang Huang, Weilin Zhao, Xinrong Zhang, Zheng Leng Thai, Kaihuo Zhang, Chongyi
368 Wang, Yuan Yao, Chenyang Zhao, Jie Zhou, Jie Cai, Zhongwu Zhai, Ning Ding, Chao Jia,
369 Guoyang Zeng, Dahai Li, Zhiyuan Liu, and Maosong Sun. Minicpm: Unveiling the potential of
370 small language models with scalable training strategies, 2024.
- 371 [19] Weilin Huang, Yu Qiao, and Xiaoou Tang. Robust scene text detection with convolution neural
372 network induced msr trees. In David Fleet, Tomas Pajdla, Bernt Schiele, and Tinne Tuytelaars,
373 editors, *Computer Vision – ECCV 2014*, pages 497–511, Cham, 2014. Springer International
374 Publishing.
- 375 [20] Max Jaderberg, Andrea Vedaldi, and Andrew Zisserman. Deep features for text spotting. In
376 David Fleet, Tomas Pajdla, Bernt Schiele, and Tinne Tuytelaars, editors, *Computer Vision –*
377 *ECCV 2014*, pages 512–528, Cham, 2014. Springer International Publishing.
- 378 [21] Justin Johnson, Bharath Hariharan, Laurens van der Maaten, Li Fei-Fei, C. Lawrence Zitnick,
379 and Ross Girshick. Clevr: A diagnostic dataset for compositional language and elementary
380 visual reasoning. In *Proceedings of the IEEE Conference on Computer Vision and Pattern*
381 *Recognition (CVPR)*, July 2017.
- 382 [22] Hugo Laurençon, Lucile Saulnier, Léo Tronchon, Stas Bekman, Amanpreet Singh, Anton
383 Lozhkov, Thomas Wang, Siddharth Karamcheti, Alexander M. Rush, Douwe Kiela, Matthieu
384 Cord, and Victor Sanh. Obelics: An open web-scale filtered dataset of interleaved image-text
385 documents, 2023.
- 386 [23] Hugo Laurençon, Léo Tronchon, Matthieu Cord, and Victor Sanh. What matters when building
387 vision-language models?, 2024.
- 388 [24] Bao Li, Chi Zhang, Long Cao, Panpan Chen, Tianyuan Liu, Hui Gao, Linyuan Wang, Bin Yan,
389 and Li Tong. Brain Functional Representation of Highly Occluded Object Recognition. *Brain*
390 *Sciences*, 13(10):1387, October 2023.
- 391 [25] Zhang Li, Biao Yang, Qiang Liu, Zhiyin Ma, Shuo Zhang, Jingxu Yang, Yabo Sun, Yuliang
392 Liu, and Xiang Bai. Monkey: Image resolution and text label are important things for large
393 multi-modal models. *arXiv preprint arXiv: 2311.06607*, 2023.
- 394 [26] Haotian Liu, Chunyuan Li, Yuheng Li, and Yong Jae Lee. Improved baselines with visual
395 instruction tuning, 2023.
- 396 [27] Haotian Liu, Chunyuan Li, Yuheng Li, Bo Li, Yuanhan Zhang, Sheng Shen, and Yong Jae Lee.
397 Llava-next: Improved reasoning, ocr, and world knowledge, January 2024.
- 398 [28] Haotian Liu, Chunyuan Li, Qingyang Wu, and Yong Jae Lee. Visual instruction tuning. In
399 *Advances in Neural Information Processing Systems*, volume 36, pages 34892–34916. Curran
400 Associates, Inc., 2023.
- 401 [29] Yuliang Liu, Biao Yang, Qiang Liu, Zhang Li, Zhiyin Ma, Shuo Zhang, and Xiang Bai.
402 Textmonkey: An ocr-free large multimodal model for understanding document. *arXiv preprint*
403 *arXiv: 2403.04473*, 2024.

- 404 [30] Haoyu Lu, Wen Liu, Bo Zhang, Bingxuan Wang, Kai Dong, Bo Liu, Jingxiang Sun, Tongzheng
405 Ren, Zhuoshu Li, Hao Yang, Yaofeng Sun, Chengqi Deng, Hanwei Xu, Zhenda Xie, and Chong
406 Ruan. Deepseek-vl: Towards real-world vision-language understanding, 2024.
- 407 [31] Pan Lu, Hritik Bansal, Tony Xia, Jiacheng Liu, Chunyuan Li, Hannaneh Hajishirzi, Hao
408 Cheng, Kai-Wei Chang, Michel Galley, and Jianfeng Gao. Mathvista: Evaluating mathematical
409 reasoning of foundation models in visual contexts. In *The Twelfth International Conference
410 on Learning Representations, ICLR 2024, Vienna, Austria, May 7-11, 2024*. OpenReview.net,
411 2024.
- 412 [32] Kenneth Marino, Mohammad Rastegari, Ali Farhadi, and Roozbeh Mottaghi. Ok-vqa: A visual
413 question answering benchmark requiring external knowledge. In *Proceedings of the IEEE/CVF
414 Conference on Computer Vision and Pattern Recognition (CVPR)*, June 2019.
- 415 [33] Minesh Mathew, Viraj Bagal, Rubèn Tito, Dimosthenis Karatzas, Ernest Valveny, and C.V.
416 Jawahar. Infographicvqa. In *Proceedings of the IEEE/CVF Winter Conference on Applications
417 of Computer Vision (WACV)*, pages 1697–1706, January 2022.
- 418 [34] Minesh Mathew, Dimosthenis Karatzas, and C.V. Jawahar. Docvqa: A dataset for vqa on
419 document images. In *Proceedings of the IEEE/CVF Winter Conference on Applications of
420 Computer Vision (WACV)*, pages 2200–2209, January 2021.
- 421 [35] Anand Mishra, Shashank Shekhar, Ajeet Kumar Singh, and Anirban Chakraborty. Ocr-vqa:
422 Visual question answering by reading text in images. In *2019 International Conference on
423 Document Analysis and Recognition (ICDAR)*, pages 947–952, 2019.
- 424 [36] Anand Mishra, Shashank Shekhar, Ajeet Kumar Singh, and Anirban Chakraborty. Ocr-vqa:
425 Visual question answering by reading text in images. In *2019 International Conference on
426 Document Analysis and Recognition (ICDAR)*, pages 947–952, 2019.
- 427 [37] G. Nagy. Twenty years of document image analysis in pami. *IEEE Transactions on Pattern
428 Analysis and Machine Intelligence*, 22(01):38–62, jan 2000.
- 429 [38] OpenAI, Josh Achiam, Steven Adler, Sandhini Agarwal, Lama Ahmad, Ilge Akkaya, Floren-
430 cia Leoni Aleman, Diogo Almeida, Janko Altenschmidt, Sam Altman, Shyamal Anadkat, Red
431 Avila, Igor Babuschkin, Suchir Balaji, Valerie Balcom, Paul Baltescu, Haiming Bao, Moham-
432 mad Bavarian, Jeff Belgum, Irwan Bello, et al. Gpt-4 technical report. *arXiv preprint arXiv:
433 2303.08774*, 2023.
- 434 [39] Long Ouyang, Jeffrey Wu, Xu Jiang, Diogo Almeida, Carroll Wainwright, Pamela Mishkin,
435 Chong Zhang, Sandhini Agarwal, Katarina Slama, Alex Ray, et al. Training language models to
436 follow instructions with human feedback. *Advances in neural information processing systems*,
437 35:27730–27744, 2022.
- 438 [40] Luiz Pessoa, Evan Thompson, and Alva Noë. Finding out about filling-in: A guide to perceptual
439 completion for visual science and the philosophy of perception. *Behavioral and Brain Sciences*,
440 21(6):723–748, 1998.
- 441 [41] Alec Radford, Jong Wook Kim, Chris Hallacy, A. Ramesh, Gabriel Goh, Sandhini Agarwal,
442 Girish Sastry, Amanda Askell, Pamela Mishkin, Jack Clark, Gretchen Krueger, and I. Sutskever.
443 Learning transferable visual models from natural language supervision. *International Confer-
444 ence on Machine Learning*, 2021.
- 445 [42] Hao Shao, Shengju Qian, Han Xiao, Guanglu Song, Zhuofan Zong, Letian Wang, Yu Liu, and
446 Hongsheng Li. Visual cot: Advancing multi-modal language models with a comprehensive
447 dataset and benchmark for chain-of-thought reasoning. *arXiv preprint arXiv: 2403.16999*, 2024.
- 448 [43] Amanpreet Singh, Vivek Natarajan, Meet Shah, Yu Jiang, Xinlei Chen, Dhruv Batra, Devi
449 Parikh, and Marcus Rohrbach. Towards vqa models that can read. In *Proceedings of the
450 IEEE/CVF conference on computer vision and pattern recognition*, pages 8317–8326, 2019.
- 451 [44] Zeyi Sun, Ye Fang, Tong Wu, Pan Zhang, Yuhang Zang, Shu Kong, Yuanjun Xiong, Dahua
452 Lin, and Jiaqi Wang. Alpha-clip: A clip model focusing on wherever you want. *arXiv preprint
453 arXiv: 2312.03818*, 2023.

- 454 [45] Gemini Team, Petko Georgiev, Ving Ian Lei, Ryan Burnell, Libin Bai, Anmol Gulati, Garrett
455 Tanzer, Damien Vincent, Zhufeng Pan, Shibo Wang, Soroosh Mariooryad, Yifan Ding, Xinyang
456 Geng, Fred Alcober, Roy Frostig, Mark Omernick, Lexi Walker, Cosmin Paduraru, Christina
457 Sorokin, Andrea Tacchetti, et al. Gemini 1.5: Unlocking multimodal understanding across
458 millions of tokens of context. *arXiv preprint arXiv: 2403.05530*, 2024.
- 459 [46] Reka Team, Aitor Ormazabal, Che Zheng, Cyprien de Masson d’Autume, Dani Yogatama, Deyu
460 Fu, Donovan Ong, Eric Chen, Eugenie Lamprecht, Hai Pham, Isaac Ong, Kaloyan Aleksiev,
461 Lei Li, Matthew Henderson, Max Bain, Mikel Artetxe, Nishant Relan, Piotr Padlewski, Qi Liu,
462 Ren Chen, Samuel Phua, Yazheng Yang, Yi Tay, Yuqi Wang, Zhongkai Zhu, and Zhihui Xie.
463 Reka core, flash, and edge: A series of powerful multimodal language models. *arXiv preprint
464 arXiv: 2404.12387*, 2024.
- 465 [47] G. Thinés, A. Costall, and G. Butterworth. *Michotte’s Experimental Phenomenology of Perception*.
466 Routledge Library Editions: Phenomenology. Taylor & Francis, 2013.
- 467 [48] Hugo Touvron, Louis Martin, Kevin Stone, Peter Albert, Amjad Almahairi, Yasmine Babaei,
468 Nikolay Bashlykov, Soumya Batra, Prajjwal Bhargava, Shruti Bhosale, Dan Bikel, Lukas
469 Blecher, Cristian Canton Ferrer, Moya Chen, Guillem Cucurull, David Esiobu, Jude Fernandes,
470 Jeremy Fu, Wenyin Fu, Brian Fuller, Cynthia Gao, Vedanuj Goswami, Naman Goyal, Anthony
471 Hartshorn, Saghar Hosseini, Rui Hou, Hakan Inan, Marcin Kardas, Viktor Kerkez, Madian
472 Khabsa, Isabel Kloumann, Artem Korenev, Punit Singh Koura, Marie-Anne Lachaux, Thibaut
473 Lavril, Jenya Lee, Diana Liskovich, Yinghai Lu, Yuning Mao, Xavier Martinet, Todor Mihaylov,
474 Pushkar Mishra, Igor Molybog, Yixin Nie, Andrew Poulton, Jeremy Reizenstein, Rashi Rungta,
475 Kalyan Saladi, Alan Schelten, Ruan Silva, Eric Michael Smith, Ranjan Subramanian, Xiao-
476 qing Ellen Tan, Binh Tang, Ross Taylor, Adina Williams, Jian Xiang Kuan, Puxin Xu, Zheng
477 Yan, Iliyan Zarov, Yuchen Zhang, Angela Fan, Melanie Kambadur, Sharan Narang, Aurelien
478 Rodriguez, Robert Stojnic, Sergey Edunov, and Thomas Scialom. Llama 2: Open foundation
479 and fine-tuned chat models. *arXiv preprint arXiv: 2307.09288*, 2023.
- 480 [49] Rob van Lier and Walter Gerbino. Perceptual completions. In *The Oxford Handbook of
481 Perceptual Organization*. Oxford University Press, 08 2015.
- 482 [50] Dongsheng Wang, Natraj Raman, Mathieu Sibue, Zhiqiang Ma, Petr Babkin, Simerjot Kaur,
483 Yulong Pei, Armineh Nourbakhsh, and Xiaomo Liu. Docllm: A layout-aware generative
484 language model for multimodal document understanding. *arXiv preprint arXiv: 2401.00908*,
485 2023.
- 486 [51] Peng Wang, Qi Wu, Chunhua Shen, Anthony Dick, and Anton van den Hengel. Fvqa: Fact-based
487 visual question answering. *IEEE Transactions on Pattern Analysis and Machine Intelligence*,
488 40(10):2413–2427, 2018.
- 489 [52] Weihan Wang, Qingsong Lv, Wenmeng Yu, Wenyi Hong, Ji Qi, Yan Wang, Junhui Ji, Zhuoyi
490 Yang, Lei Zhao, Xixuan Song, Jiazheng Xu, Bin Xu, Juanzi Li, Yuxiao Dong, Ming Ding, and
491 Jie Tang. Cogvlm: Visual expert for pretrained language models, 2023.
- 492 [53] Xinyu Wang, Yuliang Liu, Chunhua Shen, Chun Chet Ng, Canjie Luo, Lianwen Jin, Chee Seng
493 Chan, Anton van den Hengel, and Liangwei Wang. On the general value of evidence, and
494 bilingual scene-text visual question answering. In *Proceedings of the IEEE/CVF Conference on
495 Computer Vision and Pattern Recognition (CVPR)*, June 2020.
- 496 [54] Shilian Wu, Yongrui Li, and Zengfu Wang. Chinese text recognition enhanced by glyph and
497 character semantic information. *International Journal on Document Analysis and Recognition
498 (IJDAR)*, 27(1):45–56, March 2024.
- 499 [55] Yusong Wu, K. Chen, Tianyu Zhang, Yuchen Hui, Taylor Berg-Kirkpatrick, and S. Dubnov.
500 Large-scale contrastive language-audio pretraining with feature fusion and keyword-to-caption
501 augmentation. *IEEE International Conference on Acoustics, Speech, and Signal Processing*,
502 2022.
- 503 [56] Ruyi Xu, Yuan Yao, Zonghao Guo, Junbo Cui, Zanlin Ni, Chunjiang Ge, Tat-Seng Chua,
504 Zhiyuan Liu, and Gao Huang. LLaVA-UHD: an lmm perceiving any aspect ratio and high-
505 resolution images. *arXiv preprint arXiv:2403.11703*, 2024.

- 506 [57] Zhengyuan Yang, Yijuan Lu, Jianfeng Wang, Xi Yin, Dinei Florencio, Lijuan Wang, Cha Zhang,
507 Lei Zhang, and Jiebo Luo. Tap: Text-aware pre-training for text-vqa and text-caption. In
508 *Proceedings of the IEEE/CVF Conference on Computer Vision and Pattern Recognition (CVPR)*,
509 pages 8751–8761, June 2021.
- 510 [58] Tianyu Yu, Yuan Yao, Haoye Zhang, Taiwen He, Yifeng Han, Ganqu Cui, Jinyi Hu, Zhiyuan
511 Liu, Hai-Tao Zheng, Maosong Sun, et al. Rlhf-v: Towards trustworthy mllms via behavior
512 alignment from fine-grained correctional human feedback. *arXiv preprint arXiv:2312.00849*,
513 2023.
- 514 [59] Tianyu Yu, Haoye Zhang, Yuan Yao, Yunkai Dang, Da Chen, Xiaoman Lu, Ganqu Cui, Taiwen
515 He, Zhiyuan Liu, Tat-Seng Chua, and Maosong Sun. Rlaif-v: Aligning mllms through open-
516 source ai feedback for super gpt-4v trustworthiness. *arXiv preprint arXiv:2405.17220*, 2024.
- 517 [60] Xiaohua Zhai, Basil Mustafa, Alexander Kolesnikov, and Lucas Beyer. Sigmoid loss for
518 language image pre-training. *IEEE International Conference on Computer Vision*, 2023.
- 519 [61] Zhuosheng Zhang, Aston Zhang, Mu Li, Hai Zhao, G. Karypis, and Alexander J. Smola.
520 Multimodal chain-of-thought reasoning in language models. *Trans. Mach. Learn. Res.*, 2023.
- 521 [62] Yuliang Zhao, Xinyue Zhang, Boya Fu, Zhikun Zhan, Hui Sun, Lianjiang Li, and Guanglie
522 Zhang. Evaluation and recognition of handwritten chinese characters based on similarities.
523 *Applied Sciences*, 12(17), 2022.

A Additional evaluation results on first 100 and 500 test cases

Table 3: Results of various open-source and closed-source vision language models on the VCR task using the first 100 test cases. Each test case includes one or more puzzles. FT means that the model is finetuned on 16,000 samples from the VCR-wiki train dataset. The best results among the finetuned models are underlined while the best results among the models without finetuning are highlighted in bold. Subscripts provide the standard deviation obtained from bootstrap.

Language	Mode	Open/closed source	Model name	Model size	Exact match (%) \uparrow			Jaccard index (%) \uparrow		
					VI + TEI	TEI	Δ	VI + TEI	TEI	Δ
English	Easy	Closed	Claude 3 Opus	-	62.0 _{6.76}	82.0 _{6.63}	-20	78.06 _{6.24}	91.12 _{6.13}	-13.06
			Claude 3.5 Sonnet	-	70.41 _{4.46}	75.15 _{3.36}	-4.73	78.12 _{8.85}	86.5 _{5.18}	-8.4
			Gemini 1.5 Pro	-	71.01 _{3.4}	86.98 _{2.67}	-15.98	82.89 _{2.27}	94.21 _{3.32}	-11.32
			GPT-4 Turbo	-	78.47 _{0.22}	86.6 _{6.79}	-8.13	88.08 _{0.25}	94.15 _{0.2}	-6.07
			GPT-4o	-	90.91_{0.36}	95.69_{0.23}	-4.78	96.77_{0.16}	98.45_{0.06}	-1.68
			GPT-4V	-	25.36 _{0.5}	18.18 _{0.54}	7.18	35.64 _{0.22}	28.49 _{0.23}	7.15
			Qwen-VL-Max	-	82.3 _{0.19}	88.04 _{0.43}	-5.74	89.73 _{0.32}	92.55 _{0.17}	-2.82
			Reka Core	-	65.68 _{3.78}	78.11 _{3.19}	-12.43	83.14 _{2.04}	90.43 _{1.49}	-7.29
			Cambrian-1	34B	78.11 _{3.16}	82.84 _{2.86}	-4.73	87.88 _{1.97}	93.12 _{2.26}	-5.24
			CogVLM2	19B	86.39_{0.66}	84.62_{0.92}	1.78	91.39_{0.11}	91.63_{0.11}	-0.24
	Easy	Open	CogVLM2-FT	19B	94.08 _{0.2}	94.67 _{0.26}	-0.59	98.03 _{0.07}	98.22 _{0.03}	-0.2
			DeepSeek-VL	1.3B	19.53 _{0.69}	26.04 _{1.47}	-6.51	43.73 _{0.18}	48.03 _{0.16}	-4.3
			DeepSeek-VL	7B	36.09 _{1.36}	44.97 _{0.79}	-8.88	57.81 _{0.18}	61.83 _{0.33}	-4.01
			DocOwl-1.5-Omni	8B	0.59 _{0.14}	1.18 _{0.14}	-0.59	12.69 _{0.04}	13.3 _{0.06}	-0.61
			Monkey	7B	46.75 _{0.44}	48.52 _{0.41}	-1.78	67.82 _{0.22}	68.59 _{0.13}	-0.76
			Idefics2	8B	14.79 _{0.72}	26.63 _{0.37}	-11.83	34.2 _{0.37}	51.96 _{0.1}	-17.76
			InternLM-XComposer2-VL	7B	47.93 _{0.69}	47.34 _{0.57}	0.59	73.88 _{0.22}	74.58 _{0.16}	-0.7
			InternLM-XComposer2.5-VL	7B	45.56 _{3.83}	28.99 _{3.50}	16.57	67.70 _{2.79}	54.25 _{2.70}	13.45
			InternVL-V1.5	25.5B	15.38 _{0.29}	75.15 _{0.7}	-59.76	52.21 _{0.16}	85.87 _{0.29}	-33.66
			InternVL-V2	25.5B	76.92 _{3.15}	78.70 _{3.22}	-1.78	88.29 _{1.85}	89.40 _{1.83}	-1.11
	Hard	Open	InternVL-V2	40B	86.39 _{2.66}	86.98 _{2.60}	-0.59	93.51 _{1.40}	94.35 _{1.24}	-0.84
			MiniCPM-V2.5	8B	30.18 _{0.66}	36.09 _{0.34}	-5.92	53.1 _{0.18}	59.06 _{0.14}	-5.96
			MiniCPM-V2.5-FT	8B	39.05 _{0.69}	46.75 _{0.59}	-7.69	63.05 _{0.28}	69.89 _{0.33}	-6.84
			Qwen-VL	7B	47.34 _{0.44}	46.75 _{0.57}	0.59	69.19 _{0.35}	69.19 _{0.37}	-0.17
			Yi-VL	34B	1.78 _{0.16}	1.18 _{0.11}	0.59	6.21 _{0.06}	7.56 _{0.08}	-1.3
			Yi-VL	6B	2.37 _{0.13}	1.78 _{0.22}	0.59	6.24 _{0.07}	8.05 _{0.11}	-1.81
			Claude 3 Opus	-	34.01 _{1.12}	51.0 _{0.5}	-17	57.02 _{0.24}	70.32 _{0.15}	-13.31
			Claude 3.5 Sonnet	-	46.73 _{3.58}	43.2 _{3.83}	3.55	57.74 _{3.33}	54.13 _{3.51}	3.61
			Gemini 1.5 Pro	-	33.73 _{3.69}	43.79 _{3.74}	-10.06	57.09 _{2.67}	62.94 _{2.76}	-5.25
			GPT-4 Turbo	-	53.11 _{1.46}	57.42 _{0.65}	-4.31	71.75 _{0.19}	73.82 _{0.24}	-2.07
	Hard	Closed	GPT-4o	-	74.16_{0.31}	84.69_{0.31}	-10.53	86.99_{0.09}	93.19_{0.07}	-6.21
			GPT-4V	-	28.71 _{0.49}	16.27 _{0.73}	12.44	49.89 _{0.15}	33.64 _{0.16}	16.25
			Qwen-VL-Max	-	40.67 _{0.38}	55.02 _{0.46}	-14.35	61.8 _{0.19}	72.46 _{0.15}	-10.66
			Reka Core	-	7.12 _{0.01}	10.65 _{0.38}	-3.55	25.49 _{1.99}	36.78 _{2.19}	-11.29
			Cambrian-1	34B	27.81 _{3.29}	29.59 _{3.54}	-1.78	51.39 _{2.79}	54.00 _{2.76}	-2.61
			CogVLM2	19B	44.97_{0.83}	21.3_{0.47}	23.67	65.39_{0.2}	43.86_{0.27}	21.53
			CogVLM2-FT	19B	75.74 _{0.72}	67.46 _{0.64}	8.28	90.6 _{0.13}	84.26 _{0.08}	6.34
			DeepSeek-VL	1.3B	0.0 _{0.0}	0.0 _{0.0}	0	11.7 _{0.03}	10.88 _{0.06}	0.29
			DeepSeek-VL	7B	0.59 _{0.09}	1.78 _{0.17}	-1.18	16.71 _{0.11}	18.09 _{0.13}	-1.38
			Hard	Open	DocOwl-1.5-Omni	8B	0.0 _{0.0}	0.0 _{0.0}	0	7.89 _{0.05}
Monkey	7B	1.18 _{0.22}			3.56 _{0.18}	-2.37	12.66 _{0.21}	15.97 _{0.08}	-3.31	
Idefics2	8B	1.18 _{0.2}			0.59 _{0.1}	0.59	10.81 _{0.08}	11.34 _{0.12}	-0.53	
InternLM-XComposer2-VL	7B	0.0 _{0.0}			0.59 _{0.09}	-0.59	12.69 _{0.09}	14.05 _{0.11}	-1.33	
InternLM-XComposer2.5-VL	7B	0.59 _{0.58}			1.78 _{0.01}	-1.18	14.09 _{0.04}	16.57 _{0.23}	-2.48	
InternVL-V1.5	25.5B	1.78 _{0.21}			7.1 _{0.22}	-5.33	16.28 _{0.09}	26.6 _{0.14}	-10.32	
InternVL-V2	25.5B	4.73 _{1.62}			7.10 _{0.03}	-2.37	24.16 _{1.69}	26.34 _{1.97}	-2.19	
InternVL-V2	40B	12.43 _{2.54}			16.57 _{2.89}	-4.14	33.74 _{2.40}	39.51 _{2.69}	-5.76	
MiniCPM-V2.5	8B	1.18 _{0.12}			1.78 _{0.12}	-0.59	12.02 _{0.12}	12.41 _{0.07}	-0.39	
MiniCPM-V2.5-FT	8B	10.06 _{0.43}			13.02 _{0.54}	-2.96	34.67 _{0.2}	36.43 _{0.19}	-1.76	
Chinese	Easy	Closed	Claude 3 Opus	-	0.53 _{0.51}	0.53 _{0.55}	0	11.34 _{1.07}	9.14 _{0.93}	2.2
			Claude 3.5 Sonnet	-	1.6 _{0.91}	2.13 _{1.05}	-0.53	8.07 _{1.29}	9.91 _{1.48}	-1.84
			Gemini 1.5 Pro	-	0.53 _{0.56}	0.0 _{0.0}	0.53	12.94 _{1.26}	12.77 _{1.17}	0.16
			GPT-4o	-	14.89_{2.51}	21.81_{2.98}	-6.91	38.57_{2.46}	48.29_{2.43}	-9.72
			GPT-4 Turbo	-	0.53 _{0.55}	0.0 _{0.0}	0.53	11.09 _{1.05}	7.91 _{0.65}	3.58
			Qwen-VL-Max	-	5.53 _{0.19}	8.76 _{0.37}	-2.77	13.56 _{1.11}	18.5 _{1.1}	-4.97
			Reka Core	-	0.0 _{0.0}	0.0 _{0.0}	0	3.04 _{0.53}	2.42 _{0.45}	0.61
			CogVLM2-Chinese	19B	34.57_{0.66}	34.04_{1.01}	0.53	58.78_{0.13}	57.26_{0.12}	1.52
			CogVLM2-Chinese-FT	19B	60.49 _{0.74}	67.55 _{0.73}	-1.05	79.80 _{0.17}	81.78 _{0.09}	-2.3
			Easy	Open	DeepSeek-VL	1.3B	0.0 _{0.0}	0.0 _{0.0}	0	6.69 _{0.07}
DeepSeek-VL	7B	0.0 _{0.0}			0.0 _{0.0}	0	3.99 _{0.07}	6.71 _{0.02}	-2.72	
DocOwl-1.5-Omni	8B	0.0 _{0.0}			0.0 _{0.0}	0	1.23 _{0.04}	2.97 _{0.02}	-1.75	
Monkey	7B	1.06 _{0.12}			0.53 _{0.06}	0.53	9.23 _{0.08}	12.29 _{0.13}	-3.06	
InternLM-XComposer2-VL	7B	1.06 _{0.09}			0.53 _{0.07}	0.53	13.1 _{0.03}	13.26 _{0.03}	-0.16	
InternLM-XComposer2.5-VL	7B	0.00 _{0.00}			1.60 _{0.91}	-1.60	11.94 _{0.88}	16.12 _{1.24}	-4.18	
InternVL-V1.5	25.5B	4.26 _{0.28}			3.19 _{0.38}	1.06	26.9 _{0.23}	16.31 _{1.14}	10.59	
InternVL-V2	25.5B	7.45 _{1.91}			11.70 _{2.26}	-4.26	34.61 _{2.16}	31.38 _{2.34}	3.22	
InternVL-V2	40B	26.06 _{1.17}			19.15 _{2.88}	6.91	48.98 _{2.61}	41.25 _{2.57}	7.72	
MiniCPM-V2.5	8B	4.79 _{0.16}			7.45 _{0.35}	-2.66	20.38 _{0.11}	25.38 _{0.13}	-4.81	
Hard	Open	MiniCPM-V2.5-FT	8B	6.91 _{0.33}	7.98 _{0.4}	-1.06	30.9 _{0.07}	31.46 _{0.13}	-0.66	
		Qwen-VL	7B	0.0 _{0.0}	0.0 _{0.0}	0	1.41 _{0.02}	0.66 _{0.03}	0.76	
		Yi-VL	34B	0.0 _{0.0}	0.0 _{0.0}	0	4.53 _{0.03}	1.84 _{0.05}	2.69	
		Yi-VL	6B	0.0 _{0.0}	0.0 _{0.0}	0	4.73 _{0.02}	1.55 _{0.02}	3.18	
		Claude 3 Opus	-	1.06 _{0.77}	0.53 _{0.54}	0.53	9.23 _{1.04}	7.77 _{1.83}	1.45	
		Claude 3.5 Sonnet	-	0.53 _{0.51}	0.0 _{0.0}	0.53	4.11 _{0.84}	3.32 _{0.71}	0.79	
		Gemini 1.5 Pro	-	1.06 _{0.71}	1.06 _{0.77}	0	11.58 _{1.14}	13.34 _{1.2}	-1.76	
		GPT-4o	-	2.66_{1.16}	1.6_{0.92}	1.06	23.69_{1.45}	23.69_{1.48}	0	
		GPT-4 Turbo	-	0.0 _{0.0}	0.53 _{0.53}	-0.53	8.51 _{0.7}	8.02 _{0.78}	0.49	
		Qwen-VL-Max	-	1.19 _{0.12}	1.98 _{0.09}	-0.79	6.19 _{0.1}	11.09 _{0.11}	-4.9	
Hard	Closed	Reka Core	-	0.0 _{0.0}	0.0 _{0.0}	0	3.22 _{0.51}	3.62 _{0.57}	-0.4	
		CogVLM2-Chinese	19B	3.19_{0.19}	3.19_{0.32}	0	18.33_{0.14}	21.38_{0.09}	-3.05	
		CogVLM2-Chinese-FT	19B	46.81 _{0.32}	46.28 _{0.49}	0.53	66.85 _{0.39}	69.79 _{0.12}	-2.95	
		DeepSeek-VL	1.3B	0.0 _{0.0}	0.0 _{0.0}	0	6.5 _{0.03}	4.16 _{0.03}	2.34	
		DeepSeek-VL	7B	0.0 _{0.0}	0.0 _{0.0}	0	5.22 _{0.04}	7.45 _{0.06}	-2.23	
		DocOwl-1.5-Omni	8B	0.0 _{0.0}	0.0 _{0.0}	0	1.35 _{0.02}	3.57 _{0.04}	-2.23	
		Monkey	7B	0.0 _{0.0}	0.0 _{0.0}	0	6.15 _{0.11}	6.62 _{0.11}	-0.47	
		InternLM-XComposer2-VL	7B	0.0 _{0.0}	0.0 _{0.0}	0	8.17 _{0.03}	7.99 _{0.03}	0.18	
		InternLM-XComposer2.5-VL	7B	0.00 _{0.00}	0.00 _{0.00}	0.00	10.9 _{0.88}	10.54 _{0.84}	0.32	
		InternVL-V1.5	25.5B	0.0 _{0.0}	0.0 _{0.0}	0	7.0 _{0.08}	4.67 _{0.04}	3.03	
Hard	Open	InternVL-V1.5	25.5B	0.00 _{0.00}	0.53 _{0.52}	-0.53	9.85 _{0.72}	11.97 _{1.13}	-2.11	
		InternVL-V2	40B	0.53 _{0.50}	1.06 _{0.72}	-0.53	12.26 _{1.01}	13.58 _{1.20}	-1.32	
		MiniCPM-V2.5	8B	0.53 _{0.07}	0.53 _{0.07}	0	7.28 _{0.06}	7.71 _{0.06}	-0.43	
		MiniCPM-V2.5-FT	8B	1.06 _{0.08}	2.13 _{0.19}	-1.06	18.46 _{1.1}	16.42 _{0.22}	2.03	
		Qwen-VL	7B	0.0 _{0.0}	0.0 _{0.0}	0	1.1 _{0.04}	0.06 _{0.01}	1.04	
		Yi-VL	34B	0.0 _{0.0}	0.0 _{0.0}	0	4.17 _{0.04}	2.02 _{0.04}	2.15	
		Yi-VL	6B	0.0 _{0.0}						

Table 4: Results of various open-source and closed-source vision language models on the VCR task using the first 500 test cases. Each test case includes one or more puzzles. FT means the model is finetuned on 16,000 samples from the VCR-wiki train dataset. The best results among the finetuned models are underlined while the best results among the models without finetuning are highlighted in bold. Subscripts provide the standard deviation obtained from bootstrap.

Language	Mode	Open/closed source	Model name	Model size	Exact match (%) \uparrow			Jaccard index (%) \uparrow					
					VI + TEI	TEI	Δ	VI + TEI	TEI	Δ			
English	Easy	Closed	Claude 3 Opus	-	62.0 _{0.13}	77.0 _{0.5}	-15	77.6 _{0.32}	88.4 _{1.39}	-10.74			
			Claude 3.5 Sonnet	-	63.8 _{1.71}	72.8 _{1.56}	-8.94	74.6 _{1.33}	83.4 _{8.14}	-8.83			
			Gemini 1.5 Pro	-	62.7 _{3.16}	82.9 _{8.13}	-20.25	77.7 _{1.21}	91.5 _{6.76}	-13.85			
			GPT-4 Turbo	-	78.7 _{4.13}	81.9 _{4.25}	-3.2	88.5 _{4.24}	92.1 _{8.03}	-3.65			
			GPT-4V	-	91.5_{5.29}	94.5_{6.13}	-3.01	96.4_{4.11}	97.7_{6.06}	-1.32			
			Qwen-VL-Max	-	52.0 _{4.24}	37.8 _{6.22}	14.17	65.3 _{6.39}	54.1 _{3.41}	11.23			
			Reka Core	-	66.4 _{6.14}	85.5 _{3.19}	-8.74	85.7 _{1.28}	91.4 _{5.29}	-5.74			
				-		78.5 _{1.42}	-12.05	84.2 _{3.86}	90.4 _{5.7}	-6.22			
			Open	Cambrian-1	34B	76.8 _{9.152}	80.2 _{5.136}	-3.35	87.6 _{6.90}	92.4 _{2.60}	-4.76		
				CogVLM2	19B	83.1_{1.28}	79.6_{3.33}	3.48	89.4_{3.27}	88.6_{5.26}	0.79		
		CogVLM2-FT		19B	<u>92.8_{0.06}</u>	<u>92.6_{7.13}</u>	0.12	<u>97.5_{1.24}</u>	<u>97.4_{5.07}</u>	0.06			
		DeepSeek-VL		1.3B	21.8 _{6.17}	30.6 _{8.03}	-8.82	45.4 _{0.33}	52.0 _{2.73}	-6.62			
		DeepSeek-VL		7B	37.7 _{6.42}	45.4 _{7.21}	-7.7	59.0 _{7.43}	64.2 _{6.57}	-5.2			
		DocOwl-1.5-Omni		8B	0.6 _{2.06}	1.8 _{6.06}	-1.24	12.6 _{5.3}	14.0 _{9.12}	-1.44			
		Monkey		7B	47.2 _{0.2}	54.1 _{6.41}	-6.96	65.7 _{0.4}	71.1 _{7.72}	-5.47			
		Idefics2		8B	14.9 _{1.14}	29.0 _{7.2}	-14.16	31.6 _{3.3}	51.5 _{0.21}	-19.87			
		InternLM-XComposer2-VL		7B	46.0 _{9.35}	46.3 _{4.25}	-0.25	71.1 _{1.2}	71.7 _{6.67}	-0.65			
		InternLM-XComposer2.5-VL		7B	42.4 _{8.173}	25.8 _{4.53}	16.65	63.0 _{1.32}	50.7 _{5.21}	12.28			
		Hard	InternVL-V1.5	25.5B	15.7 _{8.23}	74.9 _{4.27}	-59.13	52.0 _{3.31}	86.8 _{2.47}	-34.82			
			InternVL-V2	25.5B	76.1 _{5.48}	79.1 _{3.43}	-2.98	87.6 _{3.39}	89.6 _{2.80}	-1.99			
			InternVL-V2	40B	84.8 _{4.21}	87.0 _{8.13}	-2.24	93.1 _{3.69}	94.8 _{3.59}	-1.71			
			MiniCPM-V2.5	8B	32.8 _{0.16}	36.7 _{7.25}	-3.98	52.5 _{6.25}	60.8 _{9.19}	-8.32			
			MiniCPM-V2.5-FT	8B	42.3 _{6.3}	45.3 _{4.35}	-2.98	65.3 _{9.6}	67.8 _{5.43}	-2.46			
			Qwen-VL	7B	45.4 _{7.35}	52.1 _{7.33}	-6.71	66.8 _{1.74}	71.7 _{3.59}	-4.93			
			Yi-VL	34B	48.0 _{7.06}	1.2 _{4.04}	-0.37	5.6 _{1.28}	7.6 _{3.42}	-2.02			
			Yi-VL	6B	1.1 _{2.03}	1.3 _{7.14}	-0.25	5.9 _{3.16}	7.3 _{3.23}	-1.39			
			Hard	Closed	Claude 3 Opus	-	37.8 _{0.28}	50.0 _{0.33}	-12.2	57.6 _{8.8}	70.1 _{6.64}	-12.48	
					Claude 3.5 Sonnet	-	41.7 _{4.69}	44.7 _{2.78}	-2.98	56.1 _{5.46}	58.5 _{4.16}	-2.4	
		Gemini 1.5 Pro			-	28.0 _{7.158}	38.7 _{6.68}	-10.68	51.9 _{1.22}	59.6 _{2.17}	-7.72		
		GPT-4 Turbo			-	45.1 _{5.28}	48.6 _{4.57}	-3.5	65.7 _{2.25}	67.8 _{6.2}	-2.14		
	GPT-4V	-			73.2_{0.16}	82.4_{3.017}	-9.22	86.1_{7.021}	92.0_{1.02}	-5.84			
	Qwen-VL-Max	-			25.8 _{3.44}	14.9 _{5.3}	10.87	44.6 _{3.48}	30.0 _{8.67}	14.56			
	Reka Core	-			41.6 _{5.32}	52.7 _{2.2}	-11.07	61.1 _{8.35}	70.1 _{9.37}	-9.01			
		-			6.7 _{1.89}	11.1 _{8.15}	-4.47	25.8 _{4.95}	35.8 _{3.05}	-9.99			
	Open	Cambrian-1			34B	27.2 _{0.59}	30.1 _{9.55}	-2.98	49.9 _{6.136}	55.9 _{3.23}	-5.97		
		CogVLM2			19B	41.7_{4.25}	16.7_{7.22}	24.97	62.5_{6.33}	38.4_{1.44}	24.15		
		CogVLM2-FT		19B	<u>75.3_{0.13}</u>	<u>65.2_{2.18}</u>	10.68	<u>89.7_{3.14}</u>	<u>82.7_{1.27}</u>	7.04			
		DeepSeek-VL		1.3B	0.3 _{7.02}	0.1 _{2.01}	0.25	11.4 _{2.09}	11.1 _{1.22}	0.3			
		DeepSeek-VL		7B	0.7 _{5.02}	1.6 _{1.1}	-0.87	15.8 _{2.29}	17.1 _{8.41}	-1.38			
		DocOwl-1.5-Omni		8B	0.0 _{0.0}	0.0 _{0.0}	0	7.3 _{4.06}	7.6 _{1.16}	-0.27			
		Monkey		7B	1.3 _{7.05}	2.2 _{4.15}	-0.87	13.1 _{6.18}	14.4 _{5.24}	-1.29			
		Idefics2		8B	0.6 _{2.02}	0.6 _{2.06}	0	9.2 _{4.11}	11.0 _{1.16}	-1.75			
		InternLM-XComposer2-VL		7B	0.5 _{0.4}	0.3 _{7.05}	0.12	12.3 _{8.13}	13.2 _{2.11}	-0.83			
		InternLM-XComposer2.5-VL		7B	0.7 _{5.31}	1.2 _{4.39}	-0.50	13.6 _{7.51}	14.9 _{2.56}	-1.25			
	Chinese	Easy		InternVL-V1.5	25.5B	1.7 _{4.13}	6.3 _{4.13}	-4.6	16.8 _{5.17}	26.1 _{1.24}	-9.26		
				InternVL-V2	25.5B	6.7 _{1.87}	6.7 _{1.89}	0.00	25.1 _{2.94}	24.3 _{1.96}	0.80		
				InternVL-V2	40B	14.1 _{1.22}	18.5 _{1.36}	-4.35	35.0 _{1.18}	41.0 _{2.12}	-6.02		
				MiniCPM-V2.5	8B	1.7 _{4.08}	1.6 _{1.08}	0.12	11.5 _{6.24}	11.6 _{9.38}	-0.15		
				MiniCPM-V2.5-FT	8B	11.4 _{3.11}	14.2 _{9.16}	-2.86	35.1 _{3.19}	36.6 _{5.68}	-1.52		
				Qwen-VL	7B	1.6 _{1.03}	1.7 _{4.03}	-0.12	15.2 _{8.13}	14.4 _{3.54}	0.85		
				Yi-VL	34B	0.1 _{2.01}	0.0 _{0.0}	0.12	4.3 _{1.08}	5.4 _{5.13}	-1.14		
				Yi-VL	6B	0.1 _{2.02}	0.0 _{0.0}	0.12	4.4 _{9.05}	5.7 _{6.12}	-1.21		
				Hard	Closed	Claude 3 Opus	-	0.9 _{0.3}	1.0 _{0.31}	-0.1	11.5 _{0.48}	10.0 _{0.49}	1.49
						Claude 3.5 Sonnet	-	1.0 _{0.31}	0.8 _{0.28}	0.2	7.5 _{4.24}	7.5 _{0.51}	0.03
		Gemini 1.5 Pro				-	1.1 _{0.32}	0.5 _{0.22}	0.6	11.1 _{0.56}	11.4 _{7.48}	-0.37	
		GPT-4 Turbo				-	14.8_{7.14}	22.4_{6.135}	-7.58	39.0_{5.99}	48.2_{4.09}	-9.19	
		GPT-4V	-			0.2 _{0.14}	0.1 _{0.1}	0.1	8.4 _{2.36}	6.9 _{7.29}	1.45		
		Qwen-VL-Max	-			6.3 _{4.08}	9.9 _{2.09}	-3.58	13.4 _{5.41}	22.8 _{6.46}	-9.42		
		Reka Core	-			0.0 _{0.0}	0.0 _{0.0}	0	3.4 _{3.26}	3.1 _{5.2}	0.28		
		Open	CogVLM2-Chinese			19B	33.6_{3.15}	31.4_{4.19}	2.2	57.9_{7.56}	54.0_{5.54}	3.92	
CogVLM2-Chinese-FT			19B			<u>63.9_{7.55}</u>	<u>62.6_{7.17}</u>	1.3	<u>79.7_{1.41}</u>	<u>79.2_{2.47}</u>	0.49		
DeepSeek-VL			1.3B			0.0 _{0.0}	0.0 _{0.0}	0	6.1 _{0.1}	3.2 _{5.05}	2.85		
DeepSeek-VL			7B	0.0 _{0.0}	0.0 _{0.0}	0	4.2 _{8.07}	7.3 _{6.05}	-3.02				
DocOwl-1.5-Omni			8B	0.0 _{0.0}	0.0 _{0.0}	0	1.1 _{9.05}	3.8 _{6.06}	-2.63				
Monkey	7B		0.2 _{0.1}	1.4 _{0.05}	-1.2	7.8 _{9.3}	10.2 _{6.24}	-2.37					
InternLM-XComposer2-VL	7B		0.0 _{0.05}	0.2 _{0.04}	0.4	12.3 _{4.25}	12.5 _{2.14}	-0.18					
InternLM-XComposer2.5-VL	7B		0.3 _{0.17}	0.4 _{0.20}	-0.10	12.7 _{6.42}	14.9 _{9.43}	-2.23					
InternVL-V1.5	25.5B		3.9 _{0.99}	4.6 _{9.18}	-0.7	25.8 _{6.45}	20.7 _{3.58}	5.15					
InternVL-V2	25.5B		8.0 _{8.86}	8.0 _{8.92}	0.00	32.7 _{8.89}	28.4 _{8.91}	4.31					
Hard	Closed	InternVL-V2	40B	22.7 _{5.136}	16.6 _{7.14}	6.09	49.5 _{1.06}	39.4 _{6.10}	10.05				
		MiniCPM-V2.5	8B	4.5 _{9.11}	4.8 _{9.09}	-0.3	18.1 _{2.33}	22.2 _{8.18}	-4.17				
		MiniCPM-V2.5-FT	8B	7.2 _{9.14}	7.0 _{9.12}	0.2	29.3 _{6.39}	30.6 _{7.38}	-1.31				
		Qwen-VL	7B	0.0 _{0.0}	0.0 _{0.0}	0	1.2 _{5.03}	0.4 _{3.06}	0.82				
		Yi-VL	34B	0.0 _{0.0}	0.0 _{0.0}	0	4.6 _{9.09}	1.7 _{1.06}	2.98				
		Yi-VL	6B	0.0 _{0.0}	0.0 _{0.0}	0	4.2 _{8.06}	1.6 _{6.04}	2.62				
		Open	Claude 3 Opus	-	0.3 _{0.18}	0.1 _{0.1}	0.2	9.2 _{2.38}	8.0 _{9.33}	1.13			
			Claude 3.5 Sonnet	-	0.2 _{0.15}	0.0 _{0.0}	0.2	4.0 _{3.3}	2.3 _{7.23}	1.63			
			Gemini 1.5 Pro	-	0.7 _{0.26}	0.5 _{0.23}	0.2	11.8 _{2.51}	11.7 _{5.44}	0.07			
			GPT-4 Turbo	-	2.2_{0.47}	1.8_{0.4}	0.4	22.7_{2.67}	22.8_{9.65}	-0.17			
GPT-4V	-		0.0 _{0.0}	0.2 _{0.13}	-0.2	8.5 _{8.3}	6.8 _{7.28}	1.72					
Qwen-VL-Max	-		0.8 _{9.06}	1.3 _{8.1}	-0.49	5.4 _{9.19}	12.2 _{9.18}	-6.89					
Reka Core	-		0.0 _{0.0}	0.0 _{0.0}	0	3.3 _{3.23}	2.9 _{7.2}	0.38					
Open	CogVLM2-Chinese		19B	1.2_{0.07}	2.3_{0.09}	-1.1	16.8_{3.22}	19.8_{6.23}	-3.04				
	CogVLM2-Chinese-FT		19B	<u>42.5_{1.32}</u>	<u>45.9_{1.23}</u>	-3.39	<u>65.7_{9.24}</u>	<u>69.4_{6.46}</u>	-3.68				
	DeepSeek-VL		1.3B	0.0 _{0.0}	0.0 _{0.0}	0	6.8 _{7.09}	3.5 _{3.07}	3.33				
	DeepSeek-VL	7B	0.0 _{0.0}	0.0 _{0.0}	0	5.4 _{9.07}	7.7 _{7.05}	-2.08					
	DocOwl-1.5-Omni	8B	0.0 _{0.0}	0.0 _{0.0}	0	1.6 _{8.04}	4.4 _{2.07}	-2.73					
	Monkey	7B	0.0 _{0.0}	0.0 _{0.0}	0	5.6 _{9.15}	6.3 _{3.13}	-0.61					
	InternLM-XComposer2-VL	7B	0.0 _{0.0}	0.0 _{0.0}	0	8.3 _{6.09}	7.9 _{2.09}	0.44					
	InternLM-XComposer2.5-VL	7B	0.0 _{0.00}	0.0 _{0.00}	0.00	10.8 _{3.31}	10.8 _{1.31}	0.02					
	InternVL-V1.5	25.5B	0.0 _{0.0}	0.0 _{0.0}	0	7.9 _{1.12}	6.1 _{1.26}	1.79					
	InternVL-V2	25.5B	0.0 _{0.00}	0.1 _{0.09}	-0.10	9.5 _{9.31}	10.1 _{5.39}	-0.57					
InternVL-V2	40B	0.4 _{0.20}	0.9 _{0.29}	-0.50	12.3 _{3.42}	13.8 _{3.48}	-1.50						
MiniCPM-V2.5	8B	1.2 _{0.03}	0.2 _{0.1}	0	7.2 _{3.18}	7.6 _{1.3}	-0.37						
MiniCPM-V2.5-FT	8B	1.2 _{0.03}	1.4 _{0.06}	-0.2	18.0 _{1.35}	15.2 _{5.25}	2.76						
Qwen-VL	7B	0.0 _{0.0}	0.0 _{0.0}	0	11.0 _{7.07}	0.1 _{5.01}	0.94						
Yi-VL	34B	0.0 _{0.0}	0.0 _{0.0}	0	4.4 _{9.09}	1.7 _{3.1}	2.76						
Yi-VL	6B	0.0 _{0.0}	0.0 _{0.0}	0	3.9 _{5.05}	2.0 _{8.09}	1.87						

525 We show the table of evaluation results on first 100 and 500 test cases for better comparison with
 526 human evaluation results and closed-source models correspondingly.

527 B Relationship between VCR-wiki-en and Other Benchmarks

528 We evaluate 38 VLMs across 23 benchmarks, treating the VLM scores as features of the benchmarks
 529 to calculate a correlation matrix. The heatmap of this matrix is presented in Figure 4. Based on the
 530 heatmap, we performed K-Means clustering and visualized the results in 2D in figure 5, using the
 531 first two principal components derived from the rows of the correlation matrix for each benchmark.
 532 We did not test VCR-wiki-zh for these processes due to the limited availability of VLMs that support
 533 Chinese.

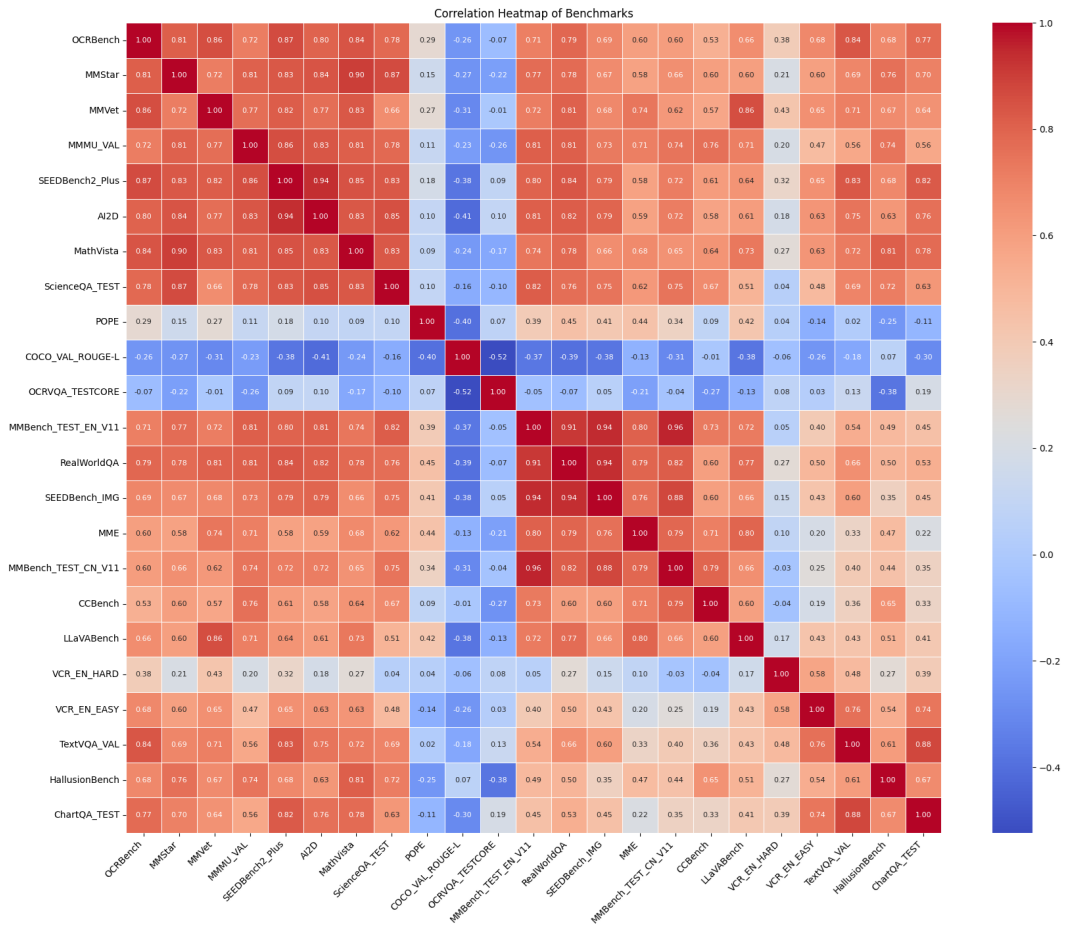


Figure 4: The heat map of benchmarks displays the correlation between the metric scores of 38 models for each benchmark pair.

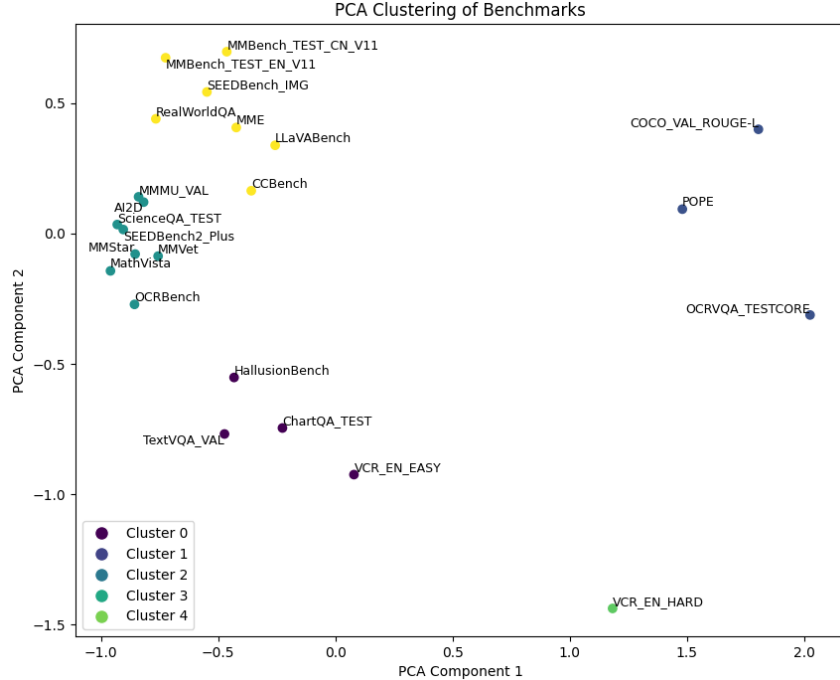


Figure 5: Each point in the figure represents the first 2 principal components of the metric score correlations between benchmarks.

534 C Dataset Creation

535 The VCR task requires aligning visual images (VI) with text embedded in images (TEI). Therefore,
 536 the dataset creation process relies on a set of highly correlated image-text pairs. We utilize the primary
 537 images and their corresponding captions from Wikipedia as the data source⁵ to create VCR-WIKI, a
 538 Wikipedia-based VCR dataset. The pipeline for creating VCR-WIKI is shown in Figure 3. Before
 539 constructing the dataset, we first filter out instances with sensitive content, including NSFW and
 540 crime-related terms, to mitigate AI risk and biases.

541 The VCR-WIKI dataset is formatted as a VQA task, where each instance includes an image, a
 542 question, and a ground-truth answer. The images are synthesized from text-image pairs by stacking
 543 the image (VI) with its corresponding text description (TEI) vertically, mimicking the format of a
 544 captioned image. This stacked image is referred to as a stacked $VI + TEI$ image. Each $VI + TEI$
 545 image is resized to a width of 300 pixels. To avoid excessive image height, we truncate TEI to a
 546 maximum of five lines. We filter the dataset to exclude instances with $VI + TEI$ images exceeding
 547 900 pixels in height to avoid drastic resolution changes during data pre-processing.

548 Within TEI , we use spaCy to randomly select several 5-grams in the caption for masking. To ensure
 549 the restoration process is doable by a human without too much professional domain knowledge, the
 550 5-grams do not contain numbers, person names, religious or political groups, facilities, organizations,
 551 locations, dates and time labeled by spaCy, and the total masked token does not exceed 50% of the
 552 tokens in the caption. We exclude all instances that do not have a single eligible 5-gram. The selected
 553 5-grams are partially obscured by a white rectangle that reveals only the upper and lower parts of
 554 the text, with the proportion of coverage varying to adjust task difficulty. Furthermore, to assess the
 555 impact of VI on model performance, we create an ablation for each image, maintaining the resolution
 556 of the $VI + TEI$ image, but retaining only the TEI part in the center of the image.

557 The VCR task involves a predefined question that prompts the model to produce the obscured text in
 558 the image. The ground truth answer corresponds to the caption displayed in the uncovered portion of
 559 the stacked image. Due to the extensive availability of vision-language models and a significant user
 560 base in both English and Chinese, we have chosen to develop the dataset in these two languages. For

⁵Datasource: https://huggingface.co/datasets/wikimedia/wit_base.

561 each language, we meticulously select the covering proportion to create two task variants: (1) an easy
 562 version, where the task is easy for native speakers but open-source OCR models almost always fail,
 563 and (2) a hard version, where the revealed part consists of only one to two pixels for the majority of
 564 letters or characters, yet the restoration task remains feasible for native speakers of the language.

565 We release the dataset under the CC BY-SA 4.0 license. We do not include the link to the dataset due
 566 to anonymity.

567 C.1 Dataset Format and Statistics

Table 5: Basic statistics of the dataset. Note that the Easy and Hard configurations for each language share the same statistics. We report the mean, standard deviation, and the 5th and 95th percentile ($\eta_{.5}$ and $\eta_{.95}$) for the stacked image height and the number of obscured text spans. Unit is in pixels.

	# Train	# Val	# Test	VI +TEI Image Height				# Obscured Text Spans			
				Mean	SD	$\eta_{.5}$	$\eta_{.95}$	Mean	SD	$\eta_{.5}$	$\eta_{.95}$
English	2095733	5000	5000	375.52	106.01	253	564	1.62	0.63	1	3
Chinese	336448	5000	5000	360.44	102.76	239	562	2.06	0.94	1	4

568 The VCR dataset comprises four configurations: English Easy, English Hard, Chinese Easy and
 569 Chinese Hard. Each configuration can be further divided into training, validation, and test splits. The
 570 validation and test splits contain 5,000 entities each. The training set for English configurations and
 571 Chinese configurations contains 2, 095, 733 and 336, 448 instances, respectively, which can be used
 572 for model continuous pretraining. We include more detailed statistics of the dataset in Table 5.

573 D Information of models evaluated

Table 6: Model specifications

Model name	Model size	Open-sourced
Claude 3 Opus	-	×
Claude 3.5 Sonnet	-	×
Gemini 1.5 Pro	-	×
GPT-4 Turbo	-	×
GPT-4o	-	×
GPT-4V	-	×
Qwen-VL-Max	-	×
Reka Core	-	×
<hr/>		
Cambrian-1 ⁶	34B	✓
CogVLM2 ⁷	19B	✓
CogVLM2-Chinese ⁸	19B	✓
DeepSeek-VL ⁹	1.3B	✓
DeepSeek-VL ¹⁰	7B	✓
Idefics2 ¹¹	8B	✓
InternLM-XComposer2-VL ¹²	7B	✓
InternVL-V1.5 ¹³	25.5B	✓
InternVL-V2 ¹⁴	25.5B	✓
InternVL-V2 ¹⁵	40B	✓
InternLM-XComposer2-VL ¹⁶	7B	✓
MiniCPM-V2.5 ¹⁷	8B	✓
Qwen-VL ¹⁸	7B	✓
Yi-VL ¹⁹	34B	✓
Yi-VL ²⁰	6B	✓
Monkey ²¹	7B	✓
DocOwl-1.5-Omni ²²	8B	✓

574 **E Potential QA**

575 **What could be the possible reason that CogVLM performs well in VCR-wiki series benchmarks?**
576 Many models we tested (DocOwl-1.5, Monkey, MiniCPM-V2.5, InternLM series, InternVL series)
577 follow a similar inference pipeline to adapt to high-resolution application scenarios:

- 578 1. An algorithm divides the input image into segments.
- 579 2. Each segment is encoded into tokens using a CILP-based image encoder.
- 580 3. A filtering mechanism (algorithm/resampler/abstractor) processes the visual tokens.
- 581 4. The filtered tokens are concatenated with language tokens and input to the LLM.

582 If, in step 3, pixel-level hints embedded in text within the image (TEL) are disregarded, the model
583 cannot correctly answer the question. Consequently, some of these models may perform better on
584 benchmarks emphasizing global features but struggle on the VCR-wiki series benchmarks, particularly
585 in the hard partitions. For example, while InternVL2-40B performs best on VCR-wiki-en-easy, it does
586 not perform well on VCR-wiki-en-hard. As noted in the paper, the easy partition of the benchmark
587 primarily verifies that the VCR task is feasible for the models, while the hard partition explores the
588 boundaries of VCR capability for both models and human test-takers (who require more time and
589 focus to solve the puzzles in the hard partition).

590 The CogVLM2 and Cambrian-1 series, by contrast, do not include step 3 in their inference pipelines.
591 Instead, their image encoders operate at mid-to-high resolutions (1K level), and they resize the input
592 image to match the supported resolution rather than dividing it into segments. The image encoder
593 resolution for CogVLM2 is 1344×1344 , while Cambrian-1 employs four image encoders, the largest
594 supporting a resolution of 1024×1024 . This approach may encounter challenges with extremely
595 shaped input images (e.g., 8192×1024), but for VCR-wiki, where images are mostly near-square (on
596 average 300×360 for VCR-wiki-zh and 300×375 for VCR-wiki-en), high-resolution support is not
597 necessary. For instance, InternLM-XComposer2-VL outperforms InternLM-XComposer2-VL-4KHD
598 on this benchmark.

599 **What could be the potential way to improve models' capability on VCR?** To suggest potential
600 avenues for improving VLM performance on VCR, we propose the following:

- 601 1. **Include VCR in VLM Pretraining:** Just as OCR parsing tasks are often included in
602 pretraining to improve OCR performance, researchers could consider incorporating VCR
603 tasks during pretraining. We have released 'vcr_transform.py' to facilitate this process,
604 making it as straightforward as data augmentation.
- 605 2. **Architectural Exploration:** CogVLM2 is the best-performing model on average across
606 the four partitions, and we believe this is largely due to its vision expert architecture.
607 We contacted the CogVLM2 team and learned that GLM-4 and CogVLM2 share the
608 same training data, yet there is a significant performance gap between them on the VCR
609 benchmarks.

⁶<https://huggingface.co/nyu-visionx/cambrian-34b>

⁷<https://huggingface.co/THUDM/CogVLM2-Llama3-chat-19B>

⁸<https://huggingface.co/THUDM/cogvlm2-llama3-Chinese-chat-19B>

⁹<https://huggingface.co/deepseek-ai/deepseek-v1-1.3b-chat>

¹⁰<https://huggingface.co/deepseek-ai/deepseek-v1-7b-chat>

¹¹<https://huggingface.co/HuggingFaceM4/Defics2-8B>

¹²<https://huggingface.co/internlm/internlm-xcomposer2-vl-7b>

¹³<https://huggingface.co/OpenGVLab/InternVL-Chat-V1-5>

¹⁴<https://huggingface.co/OpenGVLab/InternVL2-26B>

¹⁵<https://huggingface.co/OpenGVLab/InternVL2-40B>

¹⁶<https://huggingface.co/InternLM/InternLM-XComposer2-VL-7B>

¹⁷https://huggingface.co/OpenBMB/MiniCPM-Llama3-V-2_5

¹⁸<https://huggingface.co/Qwen/Qwen-VL-Chat>

¹⁹<https://huggingface.co/01-ai/Yi-VL-34B>

²⁰<https://huggingface.co/01-ai/Yi-VL-6B>

²¹<https://huggingface.co/echo840/Monkey-Chat>

²²<https://huggingface.co/mPLUG/DocOwl1.5-Omni>

610 3. **Chain-of-Thought (CoT) Methods:** Researchers could explore multi-modality pipelines
611 based on CoT techniques to improve existing VLMs on VCR tasks [8, 61]. Although a
612 model might not initially focus on the correct visual area (e.g., pixel-level hints in the TEI),
613 CoT-based techniques could help refine its focus over successive rounds.